Design, immunogenicity, and efficacy of a pan-sarbecovirus dendritic-cell targeting vaccine

Séverin Coléon, Aurélie Wiedemann, Mathieu Surénaud, Christine Lacabaratz, Sophie Hue, Mélanie Prague, Minerva Cervantes-Gonzalez, Zhiqing Wang, Jerome Ellis, Amandine Sansoni, et al.

Design, immunogenicity, and efficacy of a pan-sarbecovirus dendritic-cell targeting vaccine

Séverin Coléon[1], Aurélie Wiedemann[1¥], Mathieu Surénaud[1¥], Christine Lacabaratz[1], Sophie Hue[1,2], Mélanie Prague[1,3], Minerva Cervantes-Gonzalez[4, 5, 6], Zhiqing Wang[1,7], Jerome Ellis[1,7], Amandine Sansoni[8], Camille Pierini[8], Quentin Bardin[8], Manon Fabregue[8], Sarah Sharkaoui[8], Philippe Hoest[8], Léa Dupaty[1], Florence Picard[1], Marwa El Hajj[1], Mireille Centlivre[1], Jade Ghosn[5,6], French COVID Cohort Study Group[a], Rodolphe Thiébaut[1,9], Sylvain Cardinaud[1], Bernard Malissen[8,10], Gérard Zurawski[1,7], Ana Zarubica[8], Sandra M Zurawski[1,7], Véronique Godot[1], and Yves Lévy[1,11*]

Affiliations

1. Vaccine Research Institute, Université Paris-Est Créteil, Faculté de Médecine, INSERM U955, Team 16, Créteil, France
2. AP-HP, Hôpital Groupe Henri-Mondor Albert-Chenevier, Service d'Immunologie Biologique, Créteil, France
3. Univ. Bordeaux, Department of Public Health, Inserm Bordeaux Population Health Research Centre, Inria SISTM, UMR 1219; Bordeaux, France
4. AP-HP, Hôpital Bichat, Département Épidémiologie Biostatistiques et Recherche Clinique, INSERM, Centre d'Investigation clinique-Epidémiologie Clinique 1425 F-75018 Paris, France
5. Université de Paris, INSERM, IAME UMR 1137, F-75018 Paris, France
6. AP-HP, Hôpital Bichat, Service de Maladies Infectieuses et Tropicales, F-75018 Paris, France
7. Baylor Scott and White Research Institute, Dallas, Texas, United States of America
8. Centre d'Immunophénomique (CIPHE), Aix Marseille Université, INSERM, CNRS, CELPHEDIA, PHENOMIN, Marseille, France
9. CHU de Bordeaux, Pôle de Santé Publique, Service d'Information Médicale, Bordeaux, France

10. Centre d'Immunologie de Marseille-Luminy, Aix Marseille Université, Institut National de la Santé et de la Recherche Médicale, Centre National de la Recherche Scientifique, Marseille, France
11. Assistance Publique-Hôpitaux de Paris, Groupe Henri-Mondor Albert-Chenevier, Service Immunologie Clinique, Créteil, France

***Correspondence:** Pr. Yves Lévy, Vaccine Research Institute, INSERM U955, Hopital Henri Mondor, 51 Av Marechal de Lattre de Tassigny, 94010 Créteil, France, Phone: +33 (0) 1 49 81 44 42, Fax: +33 (0) 1 49 81 24 69, E-mail: yves.levy@aphp.fr

[¥]these authors contributed equally

[a]Members of the French COVID study group are listed in Supplementary Information

Abstract (211 words)

Background: There is an urgent need of a new generation of vaccine that are able to enhance protection against SARS-CoV-2 and related variants of concern (VOC) and emerging coronaviruses.

Methods: We identified conserved T- and B-cell epitopes from Spike (S) and Nucleocapsid (N) highly homologous to 38 sarbecoviruses, including SARS-CoV-2 VOCs, to design a protein subunit vaccine targeting antigens to Dendritic Cells (DC) via CD40 surface receptor (CD40.CoV2).

Findings: CD40.CoV2 immunization elicited high levels of cross-neutralizing antibodies against SARS-CoV-2, VOCs, and SARS-CoV-1 in K18-hACE2 transgenic mice, associated with ~~improved~~ viral control and survival after SARS-CoV-2 challenge. A direct comparison of CD40.CoV2 with the mRNA BNT162b2 vaccine showed that the two vaccines were equally immunogenic in mice. We demonstrated the potency of CD40.CoV2 to recall in vitro human multi-epitope, functional, and cytotoxic SARS-CoV-2 S- and N-specific T-cell responses that are unaffected by VOC mutations and cross-reactive with SARS-CoV-1 and, to a lesser extent, MERS epitopes.

Interpretation: We report the immunogenicity and antiviral efficacy of the CD40.CoV2 vaccine in a preclinical model providing a framework for a pan-sarbecovirus vaccine.

Fundings: This work was supported by INSERM and the Investissements d'Avenir program, Vaccine Research Institute (VRI), managed by the ANR and the CARE project funded from the Innovative Medicines Initiative 2 Joint Undertaking (JU).

Keywords: COVID-19, SARS-CoV-2, vaccine, pre-clinical model, sarbecoviruses

Word count manuscript: 9173 words

Research in context

Evidence before this study

Since the advent of effective vaccines against SARS-CoV-2 in late 2020, more than 900 publications are referenced in pubmed. In Europe, 5 vaccines are authorized: two mRNAs (Comirnaty, Spikevax), one adjuvanted protein (Nuvaxovid), two recombinant adenoviruses (Janssen, Vaxzevria). These vaccines are well tolerated, confer a protection against severe disease and hospitalization. However, all these vaccines trigger immune responses to the Spike (S) protein of SARS-CoV-2 with the aim to elicit neutralizing antibodies. Recent results from large vaccination campaigns show a waning of neutralizing antibody levels and a reduced efficacy against emergent variants of concern (VOC) characterized by the accumulation of mutations in S and Region Binding Domain (RBD) leading to escape the vaccine responses. As it has been shown that cellular immunity is of importance for long term protection and less impacted by mutations as compare to the humoral immunity, there is a global consensus for the development of a new generation of vaccines against SARS-CoV-2 and related variants and more globally against other members of the sarbecovirus family in the context of the prepardness to the next pandemic.

Added value of this study

We have developed an *in silico* process to identify sequences from S, RBD and Nucleocapsid (N) from SARS-CoV-2 highly conserved across 38 sarbecoviruses including SARS-CoV-2, related VOCs, SARS-CoV-1 and other viruses described in bats and at high risk for potential new zoonosis. We show that targeting these conserved sequences, containing a large stretch of T and B cell epitopes, to Dendritic Cells (DC) through the CD40 receptor (CD40.CoV2 vaccine) induces cross neutralizing antibodies against SARS-CoV-2, VOCs, SARS-CoV-1 and protect K18-hACE2 transgenic mice from SARS-CoV-2 challenge. We demonstrate in vitro the potency of this polyepitope-based vaccine, which contained nucleocapsid (N) antigen, to elicit polyfunctional and strong cross-reactive T cells responses unaffected by VOC mutations and to a lesser extent conserved against SARS-CoV-1. We also show the potency of this vaccine to recall cytotoxic memory T cell responses.

Implications of all the available evidence

We provide here the framework for a polyepitope-based vaccine platform. This vaccine will enrich the current *portfolio* of vaccines as a boost of preexisting immunity with the aim to extend the breadth of immune responses against current and emerging VOCs. In addition, this innovative vaccine represents an important step in preparing for future pandemics.

Introduction

Severe acute respiratory syndrome coronavirus 2 (SARS-CoV-2), which emerged in late 2019 in the Hubei province of China, has caused devastating human and economic losses worldwide. Unprecedented mobilization of the scientific community has led to the implementation of viral diagnostics, immunological monitoring tools, and the rapid development of protective vaccines.

The current landscape of COVID-19 vaccines is based on the delivery of SARS-CoV-2 Spike (S) through various vaccine platforms that elicit neutralizing-antibody responses against the S protein, including the receptor binding domain (RBD). Most of these vaccines induce Th1 responses restricted to S epitopes, depending on the type of platform and variations in the S protein [1–9], but vary in their capacity to elicit $CD8^+$ T-cell responses, known to be an important element for control of the infection. [10] Although neutralizing antibodies are a key component of a broadly protective vaccine, several recent studies have suggested that the induction of broad virus-specific $CD4^+$ and $CD8^+$ T cells could greatly augment antibody-based protection and the long-term durability of vaccine responses. [11]

Despite current progress, control of the ongoing SARS-CoV-2 pandemic is endangered by the emergence of viral variants, called variants of concern (VOC). Among them, the B.1.1.7 Alpha,[12] B.1.351 Beta,[13] P.1 Gamma,[14] B.1.617.2 Delta,[15] and recently emerged B.1.1.529 Omicron variants [16] exhibit several specific or shared mutations within the S sequences, raising substantial new concerns due to their increased transmissibility [17] and ability to escape convalescent and vaccine-induced antibody responses.[18–22] Recent studies showing a decrease in the effectiveness of mRNA vaccines against the new VOCs[23] report of breakthrough infections,[24] and concerns of reduced efficacy of vaccination in older patients [25] or immune-compromised individuals [26] highlight the need to develop a new and complementary generation of vaccines as prophylaxis or boosters that include T- and B-cell selected antigens that are potentially less affected by the mutations of VOCs.

Within the last 20 years, SARS-CoV-2 is the third major human infectious disease outbreak caused by zoonotic coronaviruses after SARS-CoV-1 in 2002-2003 and Middle East respiratory syndrome coronavirus (MERS-CoV) in 2012. The first available sequence of SARS-CoV-2 identified this novel human pathogen as a member of the *Sarbecovirus* subgenus of *Coronaviridae*[27], the same subgenus as SARS-CoV-1. The high prevalence and diversity of viruses in bats and the fact that all zoonotic sarbecoviruses identified to date use hACE2 as their entry receptor raise major concerns about a future epidemic[28–32]. These additional concerns underscore the urgent need for new vaccine candidates that are able to enhance protection against VOCs and emerging coronaviruses.

Dendritic cells (DCs) are immune system controllers that can deliver differential signals to other immune cells through intercellular interactions and soluble factors, resulting in a variety of host immune responses of varying quality. Targeting vaccine antigens to DCs via surface receptors represents an appealing strategy to improve subunit-vaccine efficacy while reducing the amount of required antigen. This strategy, which allows the delivery of designed and selected antigens, in addition to an activation signal, may also evoke a danger signal that stimulates an immune response, with or without the need of additional immune stimulants, such as adjuvants. Among the various DC receptors tested, including lectins and scavenger receptors, we previously reported the superiority of vaccines targeting diverse viral antigens to CD40-expressing antigen-presenting cells to evoke strong antigen-specific T- and B-cell responses. [33–40]

We have recently reported results on the efficacy of a new generation of subunit vaccines targeting the RBD of the SARS-CoV-2 spike protein to the CD40 receptor (aCD40.RBD). [41] We demonstrated that a single dose of the aCD40.RBD vaccine, injected without adjuvant, is sufficient to boost a rapid increase in neutralizing antibodies in convalescent non-human primates (NHPs) infected six months previously with SARS-CoV-2. Interestingly, the aCD40.RBD vaccine-elicited antibodies cross-neutralized D614G SARS-CoV-2 and the VOCs Alpha (B1.1.7) and, to a lesser extent, Beta (B1.351). This vaccination significantly

158 improved protection against a new high-dose virulent challenge versus that in non-
159 vaccinated convalescent animals.[41]

160 Drawing from this knowledge, we used *in silico* approaches to design a next-generation
161 CD40-targeting vaccine, CD40.CoV2, including T- and B-cell epitopes spanning sequences
162 from S and nucleocapsid (N) proteins from SARS-CoV-2 and highly homologous to 38
163 sarbecoviruses, including SARS-CoV-2 VOCs. We report here the immunogenicity and
164 antiviral efficacy of this vaccine in a preclinical model.
165

Methods

Ethics

Animal housing and experimental procedures were conducted according to the French and European Regulations (*Parlement Européen et du Conseil du 22 septembre 2010, Décret n° 2013-118 du 1er février 2013 relatif à la protection des animaux utilisés à des fins scientifiques*) and the National Research Council Guide for the Care and Use of Laboratory Animals (*National Research Council (U.S.), Institute for Laboratory Animal Research (U.S.), and National Academies Press (U.S.), Eds., Guide for the care and use of laboratory animals, 8th ed. Washington, D.C: National Academies Press, 2011*). The animal BSL3 facility is authorized by the French authorities (Agreement N° B 13 014 07). All animal procedures (including surgery, anesthesia, and euthanasia, as applicable) used in the current study were submitted to the Institutional Animal Care and Use Committee either of the CIPHE or Anses/ENVA/UPEC (CEEA-016) depending on the experiments and approved by the French authorities (CETEA DSV – APAFIS#26484-2020062213431976 v6 or APAFIS#25329-2020051119073072 v4, respectively). All CIPHE BSL3 facility operations are overseen by a biosecurity/biosafety officer and accredited by the Agence Nationale de Sécurité du Médicament (ANSM).

For human samples, we enrolled a subgroup of COVID-19 patients of the prospective French COVID cohort (registered at clinicaltrials.gov NCT04262921). Ethics approval was given on February 5, 2020, by the French Ethics Committee CPP-Ile-de-France VI (ID RCB: 2020-A00256-33). The study was conducted with the understanding and consent of each participant or their surrogate covering the sampling, storage, and use of biological samples.

Animals

Heterozygous K18-hACE C57BL/6J mice (strain: 2B6.Cg-Tg (K18-ACE2)2Prlmn/J) were obtained from The Jackson Laboratory. The hCD40-OST transgenic mice expressed a human *Cd40* gene in place of the mouse *Cd40* gene. They were derived at CIPHE under CIPHE-Sanofi Research Collaborative program n° 171137A10 and kindly provided by Sanofi

under the agreement MTA #209012. All breeding, genotyping, and production of hCD40/K18-hACE2 was performed at the CIPHE. The sample size was based on previous articles reporting the use of K18-hACE2 mice in SARS-CoV2 challenge experiments with 4-5 experimental units per group. Animals were housed in groups within cages and fed standard chow diets.

COVID-19 convalescent patients

Eligible patients were those who were hospitalized between March and November 2020 with virologically confirmed COVID-19. Convalescent follow-up visits were performed between one, three, and six months after infection. Patients were not vaccinated against COVID-19 at this period.

Cloning and production of the CD40.CoV2 vaccine

The vaccine was produced using the expression plasmids described in materials availability via transient transfection (TransIT-PRO® Transfection Kit, Mirus) into mammalian CHO-S cells (ThermoFisher) followed by Protein A-affinity purification.[35,42] The eluted product (2.2 mg/ml, 0.3 ng LPS/mg) was stored at -80°C in PBS with 125 mM hydroxypropyl β-cyclodextrin (Cavitron W7 HP5). CD40 binding was validated by ELISA as previously described.[36]

Wuhan/D614 SARS-CoV-2 virus production

Vero E6 cells (CRL-1586; American Type Culture Collection) were cultured at 37°C in Dulbecco's modified Eagle's medium (DMEM) supplemented with 10% fetal bovine serum (FBS), 10 mM HEPES (pH 7.3), 1 mM sodium pyruvate, 1X non-essential amino acids, and 100 U/ mL penicillin–streptomycin. The strain BetaCoV/France/IDF0372/2020 was supplied by the National Reference Centre for Respiratory Viruses hosted by the Institut Pasteur (Paris, France). The human sample from which strain BetaCoV/France/IDF0372/2020 was isolated was provided by the Bichat Hospital, Paris, France. Infectious stocks were grown by inoculating Vero E6 cells and collecting supernatants upon observation of the cytopathic

effect. Debris was removed by centrifugation and passage through a 0.22-µm filter. Supernatants were stored at -80°C.

Vaccination and infection of hCD40/K18-hACE2 transgenic mice

Mice of 8 to 12 weeks of age of both sexes received two intraperitoneal injections of the CD40.CoV2 vaccine (10 µg) plus polyinosinic-polycytidylic acid (Poly-IC; Oncovir) (50 µg) or poly(IC) alone three weeks apart. Mice were further infected with Wuhan/D614 SARS-CoV-2 at week 4. Vaccinated and mock-vaccinated mice were administered 2.5 x 10^4 PFU of SARS-CoV-2 via intranasal administration. Mice were monitored daily for morbidity (body weight) and mortality (survival). During the monitoring period, mice were scored for clinical symptoms (weight loss, eye closure, appearance of the fur, posture, and respiration). Mice obtaining a clinical score defined as reaching the experimental end-point were humanely euthanized. Blood was collected on day -2 (before vaccination), day 28 (before viral infection), and day 40 post-vaccination. Only the experimenters who injected the vaccine or the adjuvant alone were aware of the group allocation during the conduct of the experiment. The group allocation was determined according to data analysis and statistical test relevance. Two independent experiments of CD40.CoV2 vaccination followed by SARS-CoV-2 inoculation were performed (for a total of 4-5 experimental units) to minimize confounders. No animals were excluded from the study.

The clinical and immunological monitoring of Experiment 1 are reported in the manuscript and principal figures. The antibody responses monitored in Experiment 2 to confirm the main results are presented in Supplemental Figure S3.

In an independent set of experiments, the immunogenicity of the CD40.CoV2 and mRNA BNT162b2 vaccines was assessed. huCD40/K18-hACE2 and huCD40 transgenic mice received two injections of CD40.CoV2 (10 µg corresponding to 1.33 µg of antigen + poly (IC), 50 µg) or mRNA BNT162b2 (1 µg, intramuscularly) three weeks apart, respectively. Sera

were collected before immunization and one week after the second injection. No animals were excluded from the study.

Measurement of SARS-CoV-2 viral load by RT-qPCR and TCID50 (50% of tissue-culture infective dose)

For viral titration by RT-qPCR, tissues were homogenized with ceramic beads in a tissue homogenizer (Precellys – Bertin Instruments) in 0.5 mL RLT buffer. RNA was extracted using the RNeasy Mini Kit (QIAGEN) and reverse transcribed using the High-Capacity cDNA Reverse Transcription Kit (Thermo Fisher Scientific). Amplification was carried out using OneGreen Fast qPCR Premix (OZYME) according to the manufacturer's recommendations. The number of copies of the SARS-CoV-2 RNA-dependent RNA polymerase (RdRp) gene in samples was determined using the following primers: forward primer – catgtgtggcggttcactat, reverse primer – gttgtggcatctcctgatga. This region was included in a cDNA standard to allow the copy number determination down to ~100 copies per reaction. The copies of SARS-CoV-2 were compared and quantified using a standard curve and normalized to total RNA levels. An external control (mock-infected wildtype animal, nondetectable in the assay) and a positive control (SARS-CoV-2 cDNA containing the targeted region of the RdRp gene at a concentration of 10^4 copies/µl [1.94 x 10^4 copies/µl detected in the assay]) were used in the RT-qPCR analysis to validate the assay. The median tissue-culture infectious dose (TCID50) represents the dilution of a virus-containing sample at which half of the inoculated cells show signs of infection. To perform the assay, lung tissue was weighed and homogenized using ceramic beads in a tissue homogenizer (Precellys – Bertin Instruments) in 0.5 ml RPMI media supplemented with 2% FCS and 25 mM HEPES. Tissue homogenates were then clarified by centrifugation and stored at –80°C until use. Forty-thousand cells per well were seeded in 96-well plates containing 200 µl DMEM + 4% FCS and incubated for 24 h at 37°C. Tissue homogenates were serially diluted (1:10) in RPMI media and 50 µl of each dilution was transferred to the plate in six replicates for titration at five-days post-inoculation. Plates

were read for the CPE (cytopathology effect) using microscopy reader and the data were recorded. Viral titers were then calculated using the Spearman-Karber formula and expressed as TCID50/mg of tissue.

Antibody measurement

Three multiplexed MesoScale Discovery immunoassays (V-PLEX Coronavirus Panel 3, V-PLEX SARS-CoV-2 Panel 11 and V-PLEX SARS-CoV-2 Panel 22 [IgG] Kits, MesoScale Discovery, Rockville, MD, USA) were used on all available plasma samples to measure plasma IgG antibodies to SARS-CoV-2, SARS-CoV, MERS-CoV, and HCoVs. Coronavirus Panel 3 plates are MULTI-SPOT 96-well, 10 Spot, coated with three SARS-CoV-2 antigens (spike, receptor binding domain [RBD], and nucleocapsid), and spike proteins from SARS-CoV, MERS-CoV, and seasonal HCoVs OC43, HKU1, 229E, and NL63. SARS-CoV-2 Panel 11 plates are MULTI-SPOT 96-well, 10 Spot, coated with RBD proteins from various SARS-CoV-2 lineages: Wuhan; Alpha; Beta and Botswana; Gamma; Delta sub-lineages and Vietnam; Epsilon, California, and New York; Eta, Iota, India, Zeta, and Kentucky; New York; U.K. and Philippines; Kappa and India. SARS-CoV-2 Panel 22 plates are MULTI-SPOT 96-well, 10 Spot, coated with RBD proteins from various SARS-CoV-2 lineages: Wuhan; Alpha; Beta and Botswana; Gamma; Delta sub-lineages and Vietnam; Omicron sub-lineages. Assays were performed according to the manufacturer's instructions, with samples diluted 1:50 000. The electro-chemiluminescence (ECL) signal was recorded and the results are expressed as arbitrary units (AU).

Three alternative immunoassays (V-PLEX Coronavirus Panel 3, V-PLEX SARS-CoV-2 Panel 11 and V-PLEX SARS-CoV-2 Panel 22 [ACE-2] Kits, MesoScale Discovery) were used to measure the ability of mouse plasma samples to inhibit angiotensin-converting enzyme 2 (ACE2) binding to the Spike protein of different coronaviruses and different variants of SARS-CoV-2 RBD proteins. The assays were performed according to the manufacturer's instructions with samples diluted 1:33 to 1:3333. Antibody concentrations were quantified using a reference standard (ACE2 Calibration Reagent) and are expressed as units/mL (one

unit per mL concentration of ACE2 Calibration Reagent corresponds to neutralizing activity of 1 µg/mL monoclonal antibody to SARS-CoV-2 Spike protein) except for V-PLEX SARS-CoV-2 Panel 22 kit for which samples were diluted 1:200 and results were expressed in percentage of inhibition as no reference standard was included in this kit. For V-PLEX Coronavirus Panel 3, the lower limit of quantification (LLOQ) was calculated to be between 0.68 and 0.82 unit/mL for Spike CoV-2 and between 3.10 and 3.24 units/mL for Spike CoV-1. For V-PLEX SARS-CoV-2 Panel 11, the LLOQ was calculated to be between 2.83 and 2.94 units/mL for RBD Wuhan, 2.43 and 3.20 units/mL for RBD Alpha, 2.09 and 2.87 units/mL for RBD Beta, 2.56 and 2.99 units/mL for RBD Gamma, 2.01 and 3.02 units/mL for RBD Delta, and between 2.51 and 3.12 units/mL for RBD Kappa. Values under the LLOQ were imputed at the LLOQ. Thirty plasma samples from unvaccinated mice were used to determine the threshold for positivity, defined as the whole units/mL value immediately above the concentration of the highest sample for RBD (i.e., 8 units/mL) and Spike (i.e., 4 units/mL) proteins.

Specific antigens

Various peptide pools from reference strain Human 2019-nCoV HKU-SZ-005b, from JPT Peptide Technologies (Berlin, Germany) or BEI Resources, were used, as mentioned, for the various assays. A set of four pools of 15-mer peptides, overlapping by 11 amino acids, covering the four regions of S and N sequences of SARS-CoV-2 included in the CD40.CoV2 vaccine: vS1 (29 peptides), vRBD (54 peptides), vS2 (37 peptides), and vN2 (32 peptides). In certain experiments, vS1, vRBD, vS2, and vN2 were pooled to provide a combination of all sequences included in the CD40.CoV2 vaccine (vOLPmix). A pool of 54 peptides (15-mers overlapping by 11 amino acids) encompassing the three RBD mutations K417N (four peptides), E484K (three peptides), and N501Y (four peptides): RBD SARS-CoV-2 beta/gamma. Three PepMix pools of RBD SARS-CoV-2 delta, RBD SARS-CoV-2 kappa and RBD SARS-CoV-2 Omicron (15-mer peptides, overlapping by 11 amino acids). A set of two pools of 15/20-mer peptides, overlapping by 10 amino acids, covering the two regions of

RBD and N sequences of SARS-CoV-1 corresponding to the CD40.CoV2 vaccine sequences: vRBD-CoV-1 (30 peptides), vN2-CoV-1 (18 peptides). A pool of 15-mer peptides, overlapping by 11 amino acids, covering the S1 region sequence of SARS-CoV-1: S1-CoV-1 (156 peptides). A pool of 15-mer peptides, overlapping by 11 amino acids, covering the S1 region sequence of MERS: S1-MERS (168 peptides). As controls (cont.OLP), we used a set of two pools of 15-mer peptides, overlapping by 11 amino acids, of N and M sequences of SARS-CoV-2 not included in the vaccine: N1-N2 (34 peptides) and M (53 peptides) or an irrelevant pool of overlapping 15-mer peptides (11-amino acid overlaps) from the Ebola virus Mayinga variant glycoprotein (Gpz: 77 peptides).

Quantification of culture supernatant analytes

We quantified 25 analytes in supernatants from convalescent COVID-19 PBMCs on day 2 after CD40.CoV2 vaccine (1 nM), vOLP (equimolar concentration) or a control CD40 fused to the HIV Env glycoprotein 140 (strain ZM96) (CD40.Gp140z) (1nM) stimulation using the Human XL Cytokine Luminex® Performance Panel Premixed Kit: CCL2/MCP-1, CCL3/MIP-1α, CCL4/MIP-1β, CCL5/RANTES, CD40 Ligand/TNFSF5, CXCL1/GROα, CXCL10/IP-10, GCSF, Granzyme B, IFN-α, IFN-β, IFN-γ, IL-1β, IL-2, IL-4, IL-6, IL-7, IL-8/CXCL8, IL-10, IL-12 p70, IL-13, IL-17/IL-17A, PD-L1/B7-H1, TNF, and TRAIL/TNFSF10 (R&D Systems/Bio-Techne), according to the manufacturers' instructions.

Characterization of SARS-COV-2-specific immune responses in convalescent COVID-19 patients

Cellular responses to CD40.CoV2 vaccine were assessed using the Activation Induced Marker assay (AIM) and EpiMax technology.[43] For the AIM assay, PBMCs were stimulated *in vitro* with various concentrations of the CD40.CoV2 vaccine or an equimolar combination of 15-mer overlapping peptide pools covering the full-length sequence of vaccine antigens (vS1+vS2+ vRBD+vN2) referred to as vOLPmix. PBMCs (1 x 10^6) were incubated in 300 µl RPMI supplemented with 10% human serum AB (SAB) for 24 h at 37°C in 5% CO_2. T-cell activation was assessed by detection of the extracellular activation markers CD69 and

CD137, in addition to a viability marker and CD3, CD4, and CD8 to determine the T-cell lineage. For the EpiMax technology, PBMCs were stimulated *in vitro* with 1 nM CD40.CoV2 vaccine on D0 and restimulated on D8 with 1 µg/ml of various vOLPs (vS1, vRBD, vS2, or vN2). Cell functionality was assessed by intracellular cytokine staining (ICS), with Boolean gating. The flow cytometry panel included a viability marker, CD3, CD4, and CD8 to determine the T-cell lineage, and IFN-γ, TNF, and IL-2 antibodies. Distributions were plotted using SPICE version 5.22, downloaded from http://exon.niaid.nih.gov/spice.[44] T-cell proliferation was evaluated using the CellTrace™ CFSE Cell Proliferation Kit (Invitrogen) as previously described.[45] PBMCs were stimulated *in vitro* with 1 nM CD40.CoV2 vaccine or an equimolar amount of vOLPmix or 1nM CD40.Gp140z for seven days without IL-2. The medium (RPMI 10% SAB) was changed 48 h after stimulation.

Cytotoxicity assay

PBMCs from convalescent COVID-19 patients exhibiting $CD8^+$ T cell responses in Epimax assay were stimulated with 1 nM CD40.CoV2 vaccine (effector cells) or 2.5 µg/mL phytohemagglutinin-L (PHA-L) (ThermoFischer Scientific) (target-Blast cells) in RPMI 10% SAB medium replenished every 2 to 3 days with fresh medium supplemented with IL-2 (100 U/mL) (Myltenyi Biotec). After seven days, effector-$CD8^+$ T cells were isolated using a $CD8^+$ T-cell isolation kit from Myltenyi Biotec following the manufacturers' instructions and target-Blast cells were pulsed for 1 h at 37°C in 5% CO_2, either with 0.4% DMSO (control) or 2 µg/mL vOLP. After two washes, cells were labeled using various combinations of carboxyfluorescein succinimidyl ester (CFSE) (0.1 µM), Cell Trace Violet (CTV) (0.5 µM), and/or Cell Trace Far Red (CTFR) (0.02 µM) (Thermofisher Scientific) for 15 min at 37°C. Target-Blast specific populations were then mixed at a 1:1 ratio and co-cultured with effector-$CD8^+$ T-cells at various ratios in triplicate. To measure basal apoptosis, three wells were seeded with target-Blast cells alone. After a 24 h-incubation, cells were stained with LIVE/DEAD Fixable Near-IR stain (Thermofisher Scientific) and analyzed using an LSR II-3 laser flow cytometer (405, 488, and 640 nm) (Becton Dickinson). The percentage of specific

cytotoxicity among live cells was calculated as follows: specific lysis (%) = 100*[(average [count vOLP pulsed/count DMSO pulsed] target-Blast cells alone - [count vOLP pulsed/count.DMSO pulsed]) target-Blast cells + $CD8^+$ effector T cells / (average [count vOLP pulsed/count DMSO pulsed] target-Blast cells alone)].

Statistics

Graphpad Prism software version 8 was used for nonparametric statistics and plots, as described in the figure legends. Heatmaps were generated using the heatmap function from package NMF in R software, version 4.0.0. R: A language and environment for statistical computing. R Foundation for Statistical Computing, Vienna, Austria. URL: https://www.R-project.org. Statistical differences in the expression of standardized biomarkers were determined using the nonparametric Wilcoxon test, adjusting for multiple testing using the Benjamini & Hochberg correction.

Role of funders

This work was supported by INSERM and the Investissements d'Avenir program, Vaccine Research Institute (VRI), managed by the ANR under reference ANR-10-LABX-77-01 and the CARE project funded from the Innovative Medicines Initiative 2 Joint Undertaking (JU) under grant agreement No 101005077. The funding sources were not involved in the study design, data acquisition, data analysis, data interpretation, or writing of the manuscript.

Results

***In silico* down-selection of T- and B-cell polyepitope regions from SARS-CoV-2 for an improved dendritic cell-targeting vaccine platform**

We first screened three structural proteins (S, N, and M) of SARS-CoV-2 for the identification of T-cell epitopes using NetMHC 4.0 [46] and NetMHCII 2.3 [47] software, which predict peptides that bind to a large panel of class-I and -II HLAs, respectively. Linear B-cell epitopes were predicted using BepiPred 2.0.[48] We mapped a set of 9-mer epitopes binding to 80 HLA-class I molecules and 15-mer epitopes binding to 54 HLA-class II molecules, as well as all linear B-

cell epitopes. We evaluated amino-acid (aa) regions encompassing both the highest number of predicted epitopes and the largest HLA coverage. Selected regions were further screened for their sequence homology with other β coronaviruses, including SARS (designed thereafter as SARS-CoV-1), focusing on described T-cell epitopes and B-cell epitopes that generate neutralizing antibodies. Down-selected regions containing epitopes were also compared to early predicted and described SARS-CoV-2 T- and B-cell epitopes. Thus, following all ahead mentioned criteria, four designated T-and B-cell "epitope-enriched regions" were selected as vaccine (v) regions, one from N: vN2 (aa 276-411) and three from S: vS1 (aa 125-250), vRBD (aa 318-541), and vS2 (aa 1056-1209) (Figure 1a-b). These epitope-enriched regions contain a total of 640 aa with 2,313 predicted $CD8^+$ T-cell epitopes covering 100% of HLA-Class I haplotypes, 2,985 predicted $CD4^+$ T-cell epitopes covering 100% of HLA-Class II haplotypes, and 17 predicted SARS-CoV-2 linear B-cell epitopes (Figure 1 a-b, Table S1). Then, we examined whether selected vaccine sequences significantly matched so far described SARS-CoV-2 T-cell epitopes reviewed by Grifoni et al. [49] We found the vaccine sequences to contain 71/171 (42%) and 21/44 (48%) described $CD8^+$ T-cell epitopes for S and N, respectively (Table S2). These values were 57/123 (46%) and 21/53 (40%) for described $CD4^+$ T-cell epitopes (Table S3).

We then used Cobalt (https://www.ncbi.nlm.nih.gov/tools/cobalt/re_cobalt.cgi) to perform the alignment of sequences from SARS-CoV-2, four SARS-CoV-2 VOCs (α, β, γ, δ), SARS-CoV-1, and 32 recently described SARS-CoV-related coronaviruses [50–52], which include 30 viruses of bat origin and two of pangolin origin (all from the *Sarbecovirus* subgenus). Globally, the mean [min-max] percentage of homology between these 38 sarbecoviruses for vS1, vRBD, vS2, and vN2 vaccine sequences was 53.5 [36.5 to 99.2], 73.6 [63.8 to 99.6], 94.3 [86.4 to 100], and 93.5 [89.7 to 100] %, respectively (Table S4). As expected, homology between vaccine sequences and members of *Embecovirus*, *Merbecovirus*, *Setracovirus*, and *Duvinacovirus* subgenus coronaviruses was lower and varied from 6 to 38%. Beyond sequence homology across sarbecoviruses, we observed the vaccine T-cell epitopes to be

highly conserved between SARS-CoV-2 and SARS-CoV-1 and the 32 sarbecoviruses, reaching 75 to 100% homology (Tables S2 and S3). More in-depth analysis showed that among all $CD8^+$ T-cell epitopes, 62% (n = 57) differed between SARS-CoV-2 and CoV-1 by at least one mutation, but these mutations did not affect HLA-Class I binding for a large majority of them (81%), as predicted by NetMHC4.0 (Table S2). Moreover, two $CD4^+$ T-cell epitopes included in the vN2 sequence (N301-315, WPQIAQFAPSASAFF and N306-320, QFAPSASAFFGMSRI) and nine $CD8^+$ T-cell epitopes from the vS2 and vN2 sequences (S1056-1063, APHGVVFL; S1089-1096, FPREGVFV; S1137-1145, VYDPLQPEL) and vN2 (N305-314, AQFAPSASAF; N306-315, QFAPSASAF; N307-315, FAPSASAFF; 308-317, APSASAFFGM; 310-319, SASAFFGMSR; 311-319, ASAFFGMSR) were 100% homologous across all sarbecoviruses (Table S5).These results confirm that vaccine sequences, particularly vS2 and vN2, are theoretically suitable for the design of a pan-sarbecovirus vaccine aimed at eliciting broad cross-reactive specific T-cell responses.

Next, we engineered plasmids expressing the vaccine sequence vRBD fused to the C-terminus of the Heavy (H) chain of anti-human CD40 humanized 12E12 IgG4 antibody, whereas the vN2, vS1, and vS2, sequences were fused sequentially to the Light (L) chain C-terminus to generate the CD40.CoV2 vaccine (Figure 1c). We have previously shown that 12E12 anti-CD40 fused to various viral antigens enhances CD40-mediated internalization and antigen-presentation by mononuclear cells and *ex-vivo* generated monocyte-derived DCs. [36,39]

The CD40.CoV2 vaccine induces protection after viral challenge and cross-neutralizing antibody responses in the hCD40/K18-hACE2 transgenic mouse model

Transgenic mice expressing both the human (h) ACE2 receptor, the receptor of SARS-CoV-2,[53] and hCD40 receptor (hCD40/K18-hACE2) were vaccinated with two intraperitoneal injections of CD40.CoV2 vaccine (10 µg) supplemented with polyinosinic-polycytidylic acid (Poly(IC) (50 µg) three weeks apart and challenged with Wuhan/D614G SARS-CoV-2 (Figure 2a). Poly(IC) was selected as an adjuvant due to its ability to increase antigen-

presenting cell maturation.[54] In contrast to the vaccinated animals, controls exhibited significant weight loss from day 5 post-infection (pi), lasting until day 12 pi (Figure 2b). This was associated with the development of clinical symptoms in the controls from day 5 pi (Figure S1), leading to death of 67% of the animals by day 12 pi, whereas the vaccinated animals showed no symptoms and none died (Figures 2b and S1). Accordingly, the SARS-CoV-2 viral replication (genome equivalent/μg RNA) and viral infectious particles (PFU/mg of tissue) were lower in the lungs of the vaccinated mice than the controls or, indeed, undetectable (Figure 2c). We next assessed the antibody responses elicited *in vivo* by the CD40.CoV2 vaccine. One week after the booster injection (d28 post-vaccination [dpv]), the SARS-CoV-2 RBD- and S-specific IgG (Wuhan strain) binding levels were significantly higher in the vaccinated than mock-vaccinated mice ($P = 0.0004$ for both, Mann Whitney U test) (Figure 2d-2e). The CD40.CoV2 vaccine was also able to elicit RBD-specific IgG with cross-reactivity against VOCs ($\alpha, \beta, \gamma, \delta$) or the variant of interest (VOI) κ ($P = 0.0004$ for all comparisons between vaccinated and mock-vaccinated animals, Wilcoxon U test) (Figure 2d). Moreover, vaccine-elicited IgG highly cross-reacted with the SARS-CoV-1 spike protein (Figure 2e), but not the S protein of MERS or common cold coronaviruses, of which the sequences show less homology (Figure S2). By day 12 pi (corresponding to 40 dpv), cross-reactive IgG levels had increased in the control animals, but the response remained significantly lower than in the vaccinated animals ($P = 0.0238$ between vaccinated and mock-vaccinated animals, Wilcoxon U test) (Figure 2d-2e). Overall, the CD40.CoV2 vaccine elicited cross-neutralizing antibody responses against RBD from SARS-CoV-2 Wuhan and VOCs (Figure 2f) and S from both SARS-CoV-2 and SARS-CoV-1 (Figure 2g). These results were confirmed in a second replicate animal experiment (Figure S3).

In addition, the comparison of antibody responses in animals immunized either with the CD40.CoV2 and poly(IC) or mRNA BNT162b2 vaccine showed comparable levels of RBD-binding IgG (Figure 3a) and neutralizing activity (Figure 3b) against the ancestral strain (Wuhan) and $\alpha, \beta, \gamma, \delta$ VOCs. A retained activity against Omicron was observed, but with

7.2- and 9.4-fold lower binding for those raised by the CD40.CoV2 and BNT162b2 vaccines respectively, and 3.1- and 3.3-fold lower neutralizing activity (Figure 3).

In conclusion, the vaccine-elicited immune responses provided protection against SARS-CoV-2 challenge, with 100% survival, no clinical symptoms, and significant viral load control *in vivo.* These results significantly add to our previous vaccine studies in various animal models (Hu-mice, or NHP), in which aCD40 targeting vaccines were able to induce potent humoral and cellular immune responses against Influenza virus, HIV, and, more recently, SARS-CoV-2 RBD.[37,38,41,55]

The CD40.CoV2 vaccine recalls cross-reactive functional SARS-CoV-2 T-cell responses *in vitro*

We next investigated the potency of the CD40.CoV2 vaccine in recalling T-cell responses *in vitro* using PBMCs collected from individuals who had experienced a viral infection, as previously demonstrated. Peripheral blood mononuclear cells (PBMCs) from 39 convalescent COVID-19 patients (between one to six months following infection) from the French COVID cohort [56] were collected. The median [IQR] age of the patients was 56 [47-64], of whom 67% were male. First, we evaluated the frequency of $CD4^+$- and $CD8^+$-specific T cells, as assessed by the expression of the activation markers $CD69^+$ and $CD137^+$ (Figure 4a-b). [57] PBMCs (n = 5 donors) were stimulated with various doses of CD40.CoV2 vaccine, ranging from 10 to 10^{-4} nM, or an equimolar concentration of a combination of overlapping peptides (OLP) spanning the full-length sequence of the vaccine antigens (vS1+vS2+vRBD+vN2), referred as vOLPmix. The effective range of vaccine potency eliciting SARS-CoV-2-specific $CD4^+$ T cells was between 1 to 10 nM, with maximal activity at 1 nM. At these concentrations, the recall of specific $CD4^+$ T cells was 10-fold higher than with vOLPmix stimulation (Figure 4b) ($P = 0.0062$, Wilcoxon U test). We observed a similar activation profile for $CD8^+$ T cells, with the highest potency at 1 nM. Next, we confirmed the functionality of these cells, showing that the CD40.CoV2 vaccine induced robust and significantly higher proliferation of specific $CD4^+$ and $CD8^+$ T cells and $CD19^+$ B cells than cells stimulated with vOLPmix or a control

514 CD40 vaccine fused to the HIV Env glycoprotein 140 (strain ZM96) (CD40.Gp140z) (Figure
515 4c and 4d).

516 These responses were likely favored by the targeting of vaccine epitopes through the anti-
517 CD40 vehicle, as demonstrated by the broad and high levels of secretion of soluble factors
518 produced by PBMCs from convalescent COVID-19 patients (n = 15) stimulated for two days
519 with either the CD40.CoV2 vaccine (1 nM) or vOLPmix (Figure 5 and Figure S4). Vaccine
520 stimulation induced the production of chemokines involved in monocyte, macrophage, and
521 DC chemotaxis (MCP-1, IP-10), as well as those associated with T-cell (CCL5) and
522 neutrophil (IL-8) recruitment. Moreover, the level of cytokines produced by activated
523 monocytes/macrophages and DCs (TNF, MIP-1α, MIP-1β, and IL-12p70) and those specific
524 to cytotoxic activity (Granzyme B) also increased. Interestingly, Th1 (IFN-γ, IL-2), Th2 (IL-4,
525 IL-13), and Th17 (IL-17A) cytokines were also detected. By contrast, stimulation with the
526 matched vOLPmix only significantly induced the production of IL-2 (Figure 5). Moreover,
527 coculture of PBMCs with CD40.Gp140z control vaccine did not stimulate the production of
528 cytokines excluding bystander and "non-specific" activation through CD40 receptor (Figure
529 S5). Overall, these results demonstrate the potency of minute amounts of CD40.CoV2
530 vaccine to promote the recall of functional specific memory T and B cells.

531 **The CD40.CoV2 vaccine elicits multiepitope and cross-reactive specific T-cell**
532 **responses against SARS-related sequences.**

533 We next confirmed the potency of the CD40.CoV2 vaccine construct to elicit cross-reactive
534 functional memory T cells against individual vaccine regions from SARS-CoV-2 Wuhan or
535 those harboring VOC/VOI mutations within these regions and SARS-CoV-1 S1/RBD/N2
536 epitopes.

537 First, PBMCs from convalescent COVID-19 patients (M1-M6 post-infection, n = 14) were
538 stimulated with the CD40.CoV2 vaccine (1 nM) and restimulated on day 8 either with one of
539 the vOLPs (vRBD, vS1, vS2, or vN2) or control OLPs (cont.OLP), defined as SARS-CoV-2

regions either not contained in the CD40.CoV2 vaccine (SARS-CoV-2 Nucleocapsid [N1-N2] or SARS-CoV-2 Matrix [M]) or irrelevant peptides, such as Ebola glycoprotein (Gpz). The CD40.CoV2 vaccine recalled polyfunctional SARS-CoV-2-specific $CD4^+$ T cells simultaneously producing up to three cytokines (IFN-γ ± IL-2 ± TNF) (Figure 6a-c and Figure S6). Specific $CD4^+$ and, to a lesser extent, $CD8^+$ T cells produced IFN-γ against all vaccine antigens but not against control antigens (non-significant P value for control antigens vs the unstimulated condition, Wilcoxon U test). The CD40.CoV2 vaccine recalled polyepitope IFN-γ^+ responses ranked from vS1 > vRBD > vN2 > vS2 for $CD4^+$ T cells and vN2 > vRBD > vS1 for $CD8^+$ T cells (Figure 6c). We also observed significant specific TNF^+ and IL-2^+ $CD4^+$ T-cell responses against various vaccine antigens, whereas only the IL-2^+ $CD8^+$ T-cell response was significant after stimulation with vRBD (Figure S6). Interestingly, the strongest $CD8^+$ T-cell response was directed against vN2, known to be important for long-term immunity[58] (Figure 6c). Finally, vaccine-expanded specific memory $CD8^+$ T cells from five different patients showed cytotoxic activity against autologous cells pulsed with different vOLPs (vN2 or vRBD), whereas there was no cytotoxic activity when target cells were pulsed with cont.OLP (N1-N2 or M) (Figure 6d).

We also observed that CD40.CoV2 vaccine-expanded *in-vitro* $CD4^+$ and $CD8^+$ T-cell responses were not affected when the cells were stimulated with RBD OLPs containing common mutations of β/γ, δ (VOCs) and κ (VOI) (Figure 7a). Similar results were obtained when the cells were stimulated with RBD OLPs from Omicron VOC (Figure 7b).The cross-reacting $CD8^+$ and $CD4^+$ T-cell responses were polyfunctional, simultaneously producing up to 2 or 3 cytokines, respectively, with no major differences between VOCs except for Omicron where we observed a decreased polyfunctionality (Figure 7c).

Finally, we re-stimulated CD40.CoV2-stimulated PBMCs from convalescent COVID-19 patients with OLPs covering the S1 (S1-CoV-1), vRBD (vRBD-CoV-1), and vN2 (vN2-CoV-1) regions from SARS-CoV-1 and S1 from MERS. The vaccine elicited a high frequency of cross-reactive SARS-CoV-1 $CD4^+$ and $CD8^+$ T cells and, to a lower extent, cross-reactive

MERS-S1 $CD8^+$ T cells (Figure 8). Interestingly, the CD40.CoV2 vaccine-induced SARS-CoV-1- and SARS-CoV-2-specific T-cell responses were highly correlated for all corresponding antigen sequences (Figure S7). Overall, we confirm that the breadth of recall responses induced by the CD40.CoV2 vaccine is not affected by RBD mutations from SARS-CoV-2 VOCs and fully recognizes SARS-CoV-1 epitopes.

Discussion

Despite the rapid development of several effective vaccines against SARS-CoV-2, recent observations from vaccine campaigns in the general population have shown that the antibody response is waning, with reduced efficacy against VOCs. Most are characterized by mutations found in areas that are likely targeted by neutralizing antibodies, leading to vaccine escape and compromising the first line of immunological defense against SARS-CoV-2. Moreover, whether the current first-generation vaccines based on the original virus strain would still protect against emerging VOCs or pre-emergent coronaviruses, which may be responsible for future pandemics, is unknown. Thus, the development of new-generation vaccines that can induce B- and T-cell responses to a broad range of epitopes, less prone to variation, are warranted.

Here, we demonstrate the immunogenicity and anti-viral efficacy of a protein vaccine composed of three regions from S (aa 125-250, 318-541, 1056-1209) and one from N (aa 276-411) of SARS-CoV-2, accumulating a large set of predicted $CD4^+$ and $CD8^+$ T- and B-cell epitopes that are highly homologous to those of SARS-CoV-1 and 32 recently described SARS-CoV-2-related coronaviruses. The CD40.CoV2 vaccine elicited potent SARS-CoV-2-specific cross-reactive and neutralizing antibodies associated with anti-viral and protective activity against SARS-CoV-2 challenge in the hCD40/K18-hACE2 mouse model. Furthermore, vaccinated mice developed high neutralizing antibody levels against the RBD region from not only SARS-CoV-2 Wuhan but also several SARS-CoV-2 VOCs/VOI (α, β, γ, δ and κ) and S from SARS-CoV-1. These results confirm and extended our previous observations of the antiviral efficacy of the CD40.RBD vaccine in convalescent macaques.[41]

Our vaccine design was also driven by the need to include conserved epitopes to generate robust memory $CD4^+$ or $CD8^+$ T cells to provide early control of acute infection with a novel SARS-CoV-2 VOC or closely related virus in the absence of pre-existing cross-protective antibodies.[9] The *in-silico* definition of vaccine sequences was supported by several observations. First, various CD40.CoV2 vaccine epitopes have already been shown by

others, through structure-based network analysis and assessment of HLA class-I peptide stability, to be structurally constrained, thus limiting genetic variation across SARS-CoV-2, SARS-CoV-1, and sarbecoviruses.[59] For example, the CD40.CoV-2 vaccine contains 6/28 S (S319-329, RVQPTESIVRF; S321-329, QPTESIVRF; S386-395, KLNDLCFTNV; S386-396, KLNDLCFTNVY; S515-524, FELLHAPATV; S1093-1102, GVFVSNGTHW) and 6/11 N (N276-286, RRGPEQTQGNF; N305-313, AQFAPSASA; N306-314, QFAPSASAF; N306-315, QFAPSASAFF; N308-315, APSASAFF; N308-317, APSASAFFGM) of highly networked constrained regions with stabilizing $CD8^+$ T-cell epitopes with global HLA coverage. [59] Second, we showed the reactivity of $CD4^+$ and $CD8^+$ T cells to nanomolar concentrations of the CD40.CoV2 vaccine using an approach combining the expression of activation markers, cytokine production, T-cell proliferation, and cytotoxic function. These results demonstrate the immunogenicity of vaccine epitopes and are consistent with those of prior studies describing a number of them in several patient cohorts (Tables S3 and S4).[49,60–62] Third, based on the recent review of all SARS-CoV-2 $CD4^+$ and $CD8^+$ T-cell epitopes reported in 25 studies,[49] it appears that the CD40.CoV2 vaccine contains 42% of the described immunodominant $CD8^+$ T-cell epitopes for S and 39% for N. The respective values are 54% (S) and 35% (N) for the immunodominant $CD4^+$ T-cell epitopes. Moreover, all vaccine regions contain dominant epitopes. For example, the vS1 and vRBD regions of the CD40.CoV2 vaccine closely fit or overlap the two immunodominant S regions for $CD4^+$ T cells (S154-254, S296-370). Similarly, the vN2 sequence overlaps the described $CD4^+$ and $CD8^+$ T-cell immunodominant region of the nucleocapsid (201-371).[49]

A crucial question for the development of vaccines to counteract the escape of the virus from neutralizing antibodies is whether SARS-CoV-2 VOCs can evade T-cell immunity. However, even if SARS-CoV-2 does mutate, analysis of mutations associated with the various VOCs shows the vast majority of CD40.CoV2 vaccine epitopes to be conserved in SARS-CoV-2 variants (Tables S2 and S3). Accordingly, we found that *in-vitro* stimulation with the CD40.CoV-2 vaccine elicited specific cross-reactive polyfunctional $CD4^+$ and $CD8^+$ T-cell

responses against RBD from VOCs/VOI. Similarly, we found that the breadth of vaccine-elicited $CD4^+$ and $CD8^+$ T-cell responses extended to S1, RBD, and N sequences from SARS-CoV-1. Indeed, expanded $CD8^+$ T cells were even cross reactive to S1 peptides from MERS, despite low homology with SARS-CoV-2 (15%).

While it is critical to determine to what extent VOCs may or may not be susceptible to evading existing humoral responses, T-cell associated immunity is, in general, significantly more difficult for viruses to overcome, due to the broad and adaptable response generated in a given individual and because of the variety of HLA haplotypes. In this regard, the new SARS-CoV-2 B.1.1.529 (Omicron) VOC, which emerged in November 2021, is characterized by the presence of 32 mutations in Spike, located mostly in the N-terminal domain (NTD) and the RBD. Recent results have shown that this VOC significantly escapes from neutralizing antibodies, either therapeutic or those from convalescent or vaccinated individuals at various levels.[63–65] However, preliminary studies have shown minimal cross-over between mutations associated with the Omicron variant of SARS-CoV-2 and $CD8^+$ T-cell epitopes identified in convalescent COVID-19 individuals.[66] Of note, the vN2 vaccine sequence is 100% homologous with that of most VOCs, including the Omicron variant. Overall, concerning the objective to develop a vaccine with a broader range of protection, our results confirm previous observations that single amino-acid substitutions or deletions across large peptidomes do not significantly affect polyclonal memory T-cell responses.[67]

The design of the CD40.CoV-2 vaccine benefited from the high number of genetically conserved SARS-CoV-2 S and N sequences across VOCs, as well as those of SARS-CoV-related viruses, with the goal of inducing broad immune cross reactivity, a key component for the development of a next-generation pan-sarbecovirus vaccine. We show that the vaccine T-cell epitopes are highly conserved with those of SARS-CoV-2 VOCs, SARS-CoV-1, and, more generally, all 38 sarbecoviruses tested, with up to 80-100% homology for the most highly conserved T-cell epitopes (Tables S2 and S3). Moreover, we show that nine $CD8^+$ T-cell epitopes, from S and N, contained in the vaccine are 100% homologous among all

sarbecoviruses (Table S5). Globally, these results confirm that vaccine sequences, particularly vS2 and vN2, are theoretically suitable for the design of a pan-sarbecovirus vaccine aiming to elicit broad cross-reactive T-cell responses.

We further propose in this vaccination strategy to deliver the antigens through a DC-targeting platform, as the antigens were fused to a humanized anti-CD40 monoclonal antibody. This platform has already been tested *in vitro*, in various preclinical animal models, and is currently in phase I/II clinical development for a prophylactic HIV vaccine (NCT04842682). Thus, by targeting epitopes of the S and N proteins, the CD40.CoV2 vaccine may represent an excellent booster of pre-existing immunity, induced either by previous priming with available vaccines or by natural infection, as we recently demonstrated that a single dose of the CD40.RBD vaccine, injected without adjuvant, is sufficient to elicit neutralizing antibodies that protect macaques from a new viral challenge.[41]

Because SARS-CoV-2 humoral responses decline rapidly over time, repeated vaccinations at short time intervals are required to maintain high neutralizing responses, at least with the currently available vaccines, which all target the S protein.[68] However, aside from antibody responses, early induction of functional SARS-CoV-2-specific T cells is observed in patients with mild disease and rapid viral clearance.[69] In addition, recent studies have highlighted the significant cross-protective advantage of a heterologous boost, even if the vaccine antigens do not fully match the viral challenge [70] and the interest to target also conserved regions of the spike protein, outside the RBD domain, for induction of cross-neutralizing antibodies.[71] Thus, a significant advantage of our vaccine may be to extend the breadth of the responses of current vaccines.

Our study had several limitations. Due to the limited availability of hCD40/K18-hACE2 mice, we did not evaluate the potency of the CD40.CoV2 vaccine against various SARS-CoV-2 related VOCs or other sarbecovirus strains in vaccinated mice. However, we showed that the CD40.CoV2 vaccine induced binding and neutralizing IgG responses very similar or equivalent to those induced by the mRNA BNT162b2 vaccine. One potential advantage of

682 our vaccine is its capacity to elicit functional cross-reactive T-cell responses. We favored the
683 analysis of T cell responses using samples from recovered individuals instead of *in vivo*
684 preclinical models. Taking account that these responses may be dependent on the "clinical
685 history" of patients and their HLA haplotypes, they are less biased than those that would be
686 observed in an animal model. Our results show that the *in-vitro* vaccine responses are
687 directed against all vaccine proteins, which confirmed the broad HLA coverage of the vaccine
688 sequences. Although, we did not test responses against N sequences from VOC or other
689 sarbecoviruses, because of the high homology (100%) between vaccine sequences and
690 VOCs including Omicron.

691 In conclusion, it is becoming urgent to develop a "pan-sarbecovirus vaccine". The
692 development of a new protein-based vaccine with expected improved tolerability suitable for
693 people with specific vulnerabilities and children would extend the portfolio of current vaccines
694 and be instrumental in controlling the circulation of the virus and the emergence of new
695 variants. By selecting a narrow range of immunodominant epitopes, presented by a wide
696 variety of HLA alleles and less prone to genetic variations across sarbecoviruses, we provide
697 a rationale for the development of a global T cell-based vaccine to counteract emerging
698 SARS-CoV-2 variants and future SARS-like coronaviruses.

699

Contributors

Y.L, V.G, and S.C conceived and designed the study. S.Co, A.W, M.S, C.L, A.Z, B.M, Q.B, M.F, S.H, S.C, G.Z, S.Z, V.G, M.P, R.T and Y.L analyzed and interpreted the data. S.Co, M.S, L.D, F.P, A.S, C.P, Q.B, M.F, S.S, MEH and P.H performed the experiments. S.Z, Z.W, J.E, S.C, C.L, M.S., and Y.L. designed and produced the CD40.CoV2 vaccine. A.Z, B.M, and V.G supervised the animal studies. J.G and M.C.G participated in sample and clinical data collection. M.C administered the project. Y.L, V.G, S.Co, AW, M.S, A.Z, S.Z, and G.Z drafted the first version and wrote the original version of the manuscript. S.Co, A.W, V.G, C.L and Y.L verified the underlying data of the final submitted version. All authors approved the final version.

Declaration of interests

The authors S.Z., G.Z., V.G., M.C., S.C., C.L., M.S., and Y.L., are named inventors on patent applications based on this work held by Inserm Transfert. The remaining authors declare no competing interests.

Acknowledgments

We thank the patients who donated their blood. We thank F. Mentre, S. Tubiana, the French COVID cohort, and REACTing (REsearch & ACtion emergING infectious diseases) for cohort management. We thank Corinne Krief, Lydia Guillaumat, and Marie Déchenaud for the biobanking of convalescent COVID-19 patient samples. We also thank Cathleen Lutz and The Jackson Laboratory for providing the K18-hACE2 mice and Pr. Sylvie van der Werf, Dr. X.Lescure, and Pr. Y. Yazdanpanah for the BetaCoV/France/IDF0372/2020 strain. The following reagents were obtained through BEI Resources, NIAID, NIH: Peptide Array, SARS Coronavirus Nucleocapsid (N) Protein, NR-52419, and Peptide Array, SARS Coronavirus Spike (S) Protein, NR-52418. The JU receives support from the European Union's Horizon 2020 research and innovation program and EFPIA and Bill & Melinda Gates Foundation, Global Health Drug Discovery Institute, University of Dundee. The French COVID Cohort is funded through the Ministry of Health and Social Affairs and the Ministry of Higher Education

and Research dedicated COVID-19 fund, PHRC n°20-0424, and the REACTing consortium. The BetaCoV/France/IDF0372/2020 strain was supplied through the European Virus Archive goes Global (Evag) platform, a project that has received funding from the European Union's Horizon 2020 Research and Innovation Program under grant agreement N° 653316. CIPHE is supported by the Investissement d'Avenir program PHENOMIN (French National Infrastructure for mouse Phenogenomics; ANR-10-INBS-07) and DCBIOL LabEx (grants ANR-11-LABEX-0043 and ANR-10-IDEX-0001-02 PSL). This work was also supported by the Fondation pour la Recherche Médicale-ANR Flash Covid-COVI-0066 to B. Malissen (COVIDHUMICE project) and the French National Research Agency –(ANR)- Research - Action projects on Covid-19- ANR-20-COV6-0004 to V. Godot (DC-CoVac project). MEH received a master's scholarship from the EUR-LIVE Graduate School of Research "Life Trajectories and Health Vulnerability." The EUR-LIVE is a project PIA / ANR-18-EUR-0011.

Data sharing statement

The CD40.CoV2 vaccine generated in this study was deposited in GenBank: anti-human CD40 12E12 antibody IgG4 H chain (GenBank ID: AJD85779.1 residues 20-467) fused to SARS_CoV_2RBD (GenBank ID: UEP92470.1 residues 17-240) followed by EPEA (C-tag) and the anti-human CD40 12E12 antibody kappa L chain (GenBank ID: AJD85780.1 residues 21-236) fused sequentially to a linker (GenBank ID: AJD85777.1 residues 699-725), nucleocapsid phosphoprotein, partial [Severe acute respiratory syndrome coronavirus 2] (GenBank ID: QWE63393.1 residues 95-230), linker residues AR, Chain A, Spike protein S1 [Severe acute respiratory syndrome coronavirus 2] (GenBank ID: 7M8J_A residues 113-237), linker residues TR, and Sequence 12 from patent US 8518410 (Genbank ID: AGU17682.1 residues 3-27), surface glycoprotein, partial [Severe acute respiratory syndrome coronavirus 2] (GenBank ID: UET03776.1 residues 195-348). The authors declare that other data supporting the findings of this study are available from the corresponding author upon request.

References

1 Anderson EJ, Rouphael NG, Widge AT, *et al.* Safety and Immunogenicity of SARS-CoV-2 mRNA-1273 Vaccine in Older Adults. *N Engl J Med* 2020; **383**: 2427–38.

2 Angyal A, Longet S, Moore S, *et al.* T-Cell and Antibody Responses to First BNT162b2 Vaccine Dose in Previously SARS-CoV-2-Infected and Infection-Naive UK Healthcare Workers: A Multicentre, Prospective, Observational Cohort Study. *SSRN Journal* 2021. DOI:10.2139/ssrn.3812375.

3 Lozano-Ojalvo D, Camara C, Lopez-Granados E, *et al.* Differential effects of the second SARS-CoV-2 mRNA vaccine dose on T cell immunity in naive and COVID-19 recovered individuals. *Cell Reports* 2021; **36**: 109570.

4 Kalimuddin S, Qui M, Eong E, Bertoletti A, Low JG. Early T cell and binding antibody responses are associated with COVID-19 RNA vaccine efficacy onset. *OPEN ACCESS*; : 13.

5 Mazzoni A, Di Lauria N, Maggi L, *et al.* First-dose mRNA vaccination is sufficient to reactivate immunological memory to SARS-CoV-2 in subjects who have recovered from COVID-19. *Journal of Clinical Investigation* 2021; **131**: e149150.

6 Painter MM, Mathew D, Goel RR, *et al.* Rapid induction of antigen-specific CD4+ T cells is associated with coordinated humoral and cellular immune responses to SARS-CoV-2 mRNA vaccination. *Immunity* 2021; : S1074761321003083.

7 Prendecki M, Clarke C, Edwards H, *et al.* Humoral and T-cell responses to SARS-CoV-2 vaccination in patients receiving immunosuppression. *Ann Rheum Dis* 2021; : annrheumdis-2021-220626.

8 Sahin U, Muik A, Derhovanessian E, *et al.* COVID-19 vaccine BNT162b1 elicits human antibody and TH1 T cell responses. *Nature* 2020; **586**: 594–9.

9 Tarke A, Sidney J, Methot N, *et al.* Impact of SARS-CoV-2 variants on the total CD4+ and CD8+ T cell reactivity in infected or vaccinated individuals. *Cell Reports Medicine* 2021; **2**: 100355.

10 McMahan K, Yu J, Mercado NB, *et al.* Correlates of protection against SARS-CoV-2 in rhesus macaques. *Nature* 2021; **590**: 630–4.

11 Sette A, Crotty S. Adaptive immunity to SARS-CoV-2 and COVID-19. *Cell* 2021; **184**: 861–80.

12 Funk T, Pharris A, Spiteri G, *et al.* Characteristics of SARS-CoV-2 variants of concern B.1.1.7, B.1.351 or P.1: data from seven EU/EEA countries, weeks 38/2020 to 10/2021. *Eurosurveillance* 2021; **26**. DOI:10.2807/1560-7917.ES.2021.26.16.2100348.

13 Tegally H, Wilkinson E, Lessells RJ, *et al.* Sixteen novel lineages of SARS-CoV-2 in South Africa. *Nat Med* 2021; **27**: 440–6.

14 Voloch CM, Gerber AL, Leitão I de C, Galliez RM, Faffe DS. Genomic Characterization of a Novel SARS-CoV-2 Lineage from Rio de Janeiro, Brazil. *Journal of Virology* 2021; **95**: 5.

15 Cherian S, Potdar V, Jadhav S, *et al.* Convergent evolution of SARS-CoV-2 spike mutations, L452R, E484Q and P681R, in the second wave of COVID-19 in Maharashtra, India. Molecular Biology, 2021 DOI:10.1101/2021.04.22.440932.

16 Karim SSA, Karim QA. Omicron SARS-CoV-2 variant: a new chapter in the COVID-19 pandemic. *The Lancet* 2021; **398**: 2126–8.

17 Davies NG, Abbott S, Barnard RC, *et al.* Estimated transmissibility and impact of SARS-CoV-2 lineage B.1.1.7 in England. *Science* 2021; **372**: eabg3055.

18 Garcia-Beltran WF, Lam EC, St. Denis K, *et al.* Multiple SARS-CoV-2 variants escape neutralization by vaccine-induced humoral immunity. *Cell* 2021; **184**: 2372-2383.e9.

19 Hoffmann M, Arora P, Groß R, *et al.* SARS-CoV-2 variants B.1.351 and P.1 escape from neutralizing antibodies. *Cell* 2021; **184**: 2384-2393.e12.

20 Madhi SA, Baillie V, Cutland CL, *et al.* Efficacy of the ChAdOx1 nCoV-19 Covid-19 Vaccine against the B.1.351 Variant. *N Engl J Med* 2021; **384**: 1885–98.

21 Wang P, Nair MS, Liu L, *et al.* Antibody resistance of SARS-CoV-2 variants B.1.351 and B.1.1.7. *Nature* 2021; **593**: 130–5.

22 Wibmer CK, Ayres F, Hermanus T, *et al.* SARS-CoV-2 501Y.V2 escapes neutralization by South African COVID-19 donor plasma. *Nat Med* 2021; **27**: 622–5.

23 Puranik A, Lenehan PJ, Silvert E, *et al.* Comparison of two highly-effective mRNA vaccines for COVID-19 during periods of Alpha and Delta variant prevalence. ; : 29.

24 Kustin T, Harel N, Finkel U, *et al.* Evidence for increased breakthrough rates of SARS-CoV-2 variants of concern in BNT162b2-mRNA-vaccinated individuals. *Nat Med* 2021; **27**: 1379–84.

25 Israel A, Merzon E, Schäffer AA, *et al.* Elapsed time since BNT162b2 vaccine and risk of SARS-CoV-2 infection in a large cohort. Infectious Diseases (except HIV/AIDS), 2021 DOI:10.1101/2021.08.03.21261496.

26 Hadjadj J, Planas D, Ouedrani A, *et al.* Immunogenicity of BNT162b2 vaccine Against the Alpha and Delta Variants in Immunocompromised Patients. Infectious Diseases (except HIV/AIDS), 2021 DOI:10.1101/2021.08.08.21261766.

27 Wu F, Zhao S, Yu B, *et al.* A new coronavirus associated with human respiratory disease in China. *Nature* 2020; **579**: 265–9.

28 Menachery VD, Yount BL, Debbink K, *et al.* A SARS-like cluster of circulating bat coronaviruses shows potential for human emergence. *Nat Med* 2015; **21**: 1508–13.

29 Menachery VD, Yount BL, Sims AC, *et al.* SARS-like WIV1-CoV poised for human emergence. *Proc Natl Acad Sci USA* 2016; **113**: 3048–53.

30 Boni MF, Lemey P, Jiang X, *et al.* Evolutionary origins of the SARS-CoV-2 sarbecovirus lineage responsible for the COVID-19 pandemic. *Nat Microbiol* 2020; **5**: 1408–17.

31 Cohen J. The dream vaccine. *Science* 2021; **372**: 227–31.

32 Frutos R, Serra-Cobo J, Pinault L, Lopez Roig M, Devaux CA. Emergence of Bat-Related Betacoronaviruses: Hazard and Risks. *Front Microbiol* 2021; **12**: 591535.

33 Bouteau A, Kervevan J, Su Q, *et al.* DC Subsets Regulate Humoral Immune Responses by Supporting the Differentiation of Distinct Tfh Cells. *Front Immunol* 2019; **10**: 1134.

34 Chatterjee B, Smed-Sörensen A, Cohn L, *et al.* Internalization and endosomal degradation of receptor-bound antigens regulate the efficiency of cross presentation by human dendritic cells. *Blood* 2012; **120**: 2011–20.

35 Cheng L, Wang Q, Li G, *et al.* TLR3 agonist and CD40-targeting vaccination induces immune responses and reduces HIV-1 reservoirs. *Journal of Clinical Investigation* 2018; **128**: 4387–96.

36 Flamar A-L, Xue Y, Zurawski SM, *et al.* Targeting concatenated HIV antigens to human CD40 expands a broad repertoire of multifunctional CD4+ and CD8+ T cells. *AIDS* 2013; **27**: 2041–51.

37 Flamar A-L, Bonnabau H, Zurawski S, *et al.* HIV-1 T cell epitopes targeted to Rhesus macaque CD40 and DCIR: A comparative study of prototype dendritic cell targeting therapeutic vaccine candidates. *PLoS ONE* 2018; **13**: e0207794.

38 Godot V, Tcherakian C, Gil L, *et al.* TLR-9 agonist and CD40-targeting vaccination induces HIV-1 envelope-specific B cells with a diversified immunoglobulin repertoire in humanized mice. *PLoS Pathog* 2020; **16**: e1009025.

39 Yin W, Gorvel L, Zurawski S, *et al.* Functional Specialty of CD40 and Dendritic Cell Surface Lectins for Exogenous Antigen Presentation to CD8+ and CD4+ T Cells. *EBioMedicine* 2016; **5**: 46–58.

40 Zurawski G, Shen X, Zurawski S, *et al.* Superiority in Rhesus Macaques of Targeting HIV-1 Env gp140 to CD40 versus LOX-1 in Combination with Replication-Competent NYVAC-KC for Induction of Env-Specific Antibody and T Cell Responses. *J Virol* 2017; **91**. DOI:10.1128/JVI.01596-16.

41 Marlin R, Godot V, Cardinaud S, *et al.* Targeting SARS-CoV-2 receptor-binding domain to cells expressing CD40 improves protection to infection in convalescent macaques. *Nat Commun* 2021; **12**: 5215.

42 Ceglia V, Zurawski S, Montes M, *et al.* Anti-CD40 Antibodies Fused to CD40 Ligand Have Superagonist Properties. *JI* 2021; **207**: 2060–76.

43 Chujo D, Foucat E, Nguyen T-S, Chaussabel D, Banchereau J, Ueno H. ZnT8-Specific CD4+ T Cells Display Distinct Cytokine Expression Profiles between Type 1 Diabetes Patients and Healthy Adults. *PLoS ONE* 2013; **8**: e55595.

44 Roederer M, Nozzi JL, Nason MC. SPICE: Exploration and analysis of post-cytometric complex multivariate datasets. *Cytometry* 2011; **79A**: 167–74.

45 Tario JD, Muirhead KA, Pan D, Munson ME, Wallace PK. Tracking Immune Cell Proliferation and Cytotoxic Potential Using Flow Cytometry. In: Hawley TS, Hawley RG, eds. Flow Cytometry Protocols. Totowa, NJ: Humana Press, 2011: 119–64.

46 Andreatta M, Nielsen M. Gapped sequence alignment using artificial neural networks: application to the MHC class I system. *Bioinformatics* 2016; **32**: 511–7.

47 Jensen KK, Andreatta M, Marcatili P, *et al.* Improved methods for predicting peptide binding affinity to MHC class II molecules. *Immunology* 2018; **154**: 394–406.

48 Jespersen MC, Peters B, Nielsen M, Marcatili P. BepiPred-2.0: improving sequence-based B-cell epitope prediction using conformational epitopes. *Nucleic Acids Research* 2017; **45**: W24–9.

875 49 Grifoni A, Sidney J, Vita R, *et al.* SARS-CoV-2 human T cell epitopes: Adaptive immune
876 response against COVID-19. *Cell Host & Microbe* 2021; **29**: 1076–92.

877 50 Lam TT-Y, Jia N, Zhang Y-W, *et al.* Identifying SARS-CoV-2-related coronaviruses in
878 Malayan pangolins. *Nature* 2020; **583**: 282–5.

879 51 Zhou P, Yang X-L, Wang X-G, *et al.* A pneumonia outbreak associated with a new
880 coronavirus of probable bat origin. *Nature* 2020; **579**: 270–3.

881 52 Wacharapluesadee S, Tan CW, Maneeorn P, *et al.* Evidence for SARS-CoV-2 related
882 coronaviruses circulating in bats and pangolins in Southeast Asia. *Nat Commun* 2021; **12**:
883 972.

884 53 Hoffmann M, Kleine-Weber H, Schroeder S, *et al.* SARS-CoV-2 Cell Entry Depends on
885 ACE2 and TMPRSS2 and Is Blocked by a Clinically Proven Protease Inhibitor. *Cell* 2020;
886 **181**: 271-280.e8.

887 54 Cheng L, Zhang Z, Li G, *et al.* Human innate responses and adjuvant activity of TLR
888 ligands in vivo in mice reconstituted with a human immune system. *Vaccine* 2017; **35**:
889 6143–53.

890 55 Graham JP, Authie P, Yu CI, *et al.* Targeting dendritic cells in humanized mice receiving
891 adoptive T cells via monoclonal antibodies fused to Flu epitopes. *Vaccine* 2016; **34**: 4857–
892 65.

893 56 Yazdanpanah Y, French COVID cohort investigators and study group, Diallo A, *et al.*
894 Impact on disease mortality of clinical, biological, and virological characteristics at hospital
895 admission and overtime in COVID-19 patients. *J Med Virol* 2021; **93**: 2149–59.

896 57 Weiskopf D, Schmitz KS, Raadsen MP, *et al.* Phenotype and kinetics of SARS-CoV-2–
897 specific T cells in COVID-19 patients with acute respiratory distress syndrome. *Sci*
898 *Immunol* 2020; **5**: eabd2071.

899 58 Lineburg KE, Grant EJ, Swaminathan S, *et al.* CD8+ T cells specific for an
900 immunodominant SARS-CoV-2 nucleocapsid epitope cross-react with selective seasonal
901 coronaviruses. *Immunity* 2021; **54**: 1055-1065.e5.

902 59 Nathan A, Rossin EJ, Kaseke C, *et al.* Structure-guided T cell vaccine design for SARS-
903 CoV-2 variants and sarbecoviruses. *Cell* 2021; **184**: 4401-4413.e10.

904 60 Grifoni A, Weiskopf D, Ramirez SI, *et al.* Targets of T Cell Responses to SARS-CoV-2
905 Coronavirus in Humans with COVID-19 Disease and Unexposed Individuals. *Cell* 2020;
906 **181**: 1489-1501.e15.

907 61 Le Bert N, Tan AT, Kunasegaran K, *et al.* SARS-CoV-2-specific T cell immunity in cases
908 of COVID-19 and SARS, and uninfected controls. *Nature* 2020; **584**: 457–62.

909 62 Li T, Xie J, He Y, *et al.* Long-Term Persistence of Robust Antibody and Cytotoxic T Cell
910 Responses in Recovered Patients Infected with SARS Coronavirus. *PLoS ONE* 2006; **1**:
911 e24.

912 63 Cele S, Jackson L, Khoury DS, *et al.* Omicron extensively but incompletely escapes Pfizer
913 BNT162b2 neutralization. *Nature* 2021; : d41586-021-03824–5.

914 64 Planas D, Saunders N, Maes P, *et al.* Considerable escape of SARS-CoV-2 Omicron to
915 antibody neutralization. *Nature* 2021; : d41586-021-03827–2.

65 Rössler A, Riepler L, Bante D, Laer D von, Kimpel J. SARS-CoV-2 B.1.1.529 variant (Omicron) evades neutralization by sera from vaccinated and convalescent individuals. Infectious Diseases (except HIV/AIDS), 2021 DOI:10.1101/2021.12.08.21267491.

66 Redd AD, Nardin A, Kared H, *et al.* Minimal cross-over between mutations associated with Omicron variant of SARS-CoV-2 and CD8+ T cell epitopes identified in COVID-19 convalescent individuals. Immunology, 2021 DOI:10.1101/2021.12.06.471446.

67 Tarke A, Sidney J, Kidd CK, *et al.* Comprehensive analysis of T cell immunodominance and immunoprevalence of SARS-CoV-2 epitopes in COVID-19 cases. *Cell Reports Medicine* 2021; **2**: 100204.

68 Barda N, Dagan N, Cohen C, *et al.* Effectiveness of a third dose of the BNT162b2 mRNA COVID-19 vaccine for preventing severe outcomes in Israel: an observational study. *The Lancet* 2021; **398**: 2093–100.

69 Tan AT, Linster M, Tan CW, *et al.* Early induction of functional SARS-CoV-2-specific T cells associates with rapid viral clearance and mild disease in COVID-19 patients. *Cell Reports* 2021; **34**: 108728.

70 Dangi T, Palacio N, Sanchez S, *et al.* Cross-protective immunity following coronavirus vaccination and coronavirus infection. *Journal of Clinical Investigation* 2021; **131**: e151969.

71 Cameroni E, Bowen JE, Rosen LE, Saliba C, Zepeda SK, Culap K. 1 Broadly neutralizing antibodies overcome SARS-CoV-2 Omicron 2 antigenic shift. ; : 53.

72 Ward JH. Hierarchical Grouping to Optimize an Objective Function. *Journal of the American Statistical Association* 1963; **58**: 236–44.

Figure legends

Figure 1. Selection of SARS-CoV-2 T- and B-cell polyepitope regions for an improved dendritic cell-targeting vaccine platform. (a) Mapping of selected SARS-CoV-2 epitope-enriched regions. (1) Four selected vaccine regions. (2) Predicted SARS-CoV-2 $CD8^+$ T-cell epitopes (NetMHC 4.0). (3) Described SARS-CoV-2 $CD8^+$ T-cell epitopes at the time of vaccine region selection. (4) Predicted SARS-CoV-2 $CD4^+$ T-cell epitopes (NetMHCII 2.3). (5) Described SARS-CoV-2 $CD4^+$ T-cell epitopes at the time of vaccine region selection. (6) Predicted linear B-cell epitopes (BepiPred 2.0). (7) Described SARS-CoV-2 IgM, IgA, and IgG epitopes at the time of vaccine region selection. (b) Vaccine (v) regions (vS1, vRBD, vS2 and vN2) and control region not included in the vaccine (N1-N2) and (c) CD40.CoV2 vaccine construct.

Figure 2. CD40.CoV2-vaccinated animals survive SARS-CoV-2 infection and show neutralizing and cross-reactive antibody responses. (a) Design of the CD40.CoV2 vaccination strategy before SARS-CoV-2 infection. (b) Relative weight and survival of mock-vaccinated (grey) and vaccinated (blue) hCD40/K18-hACE2 transgenic mice after SARS-CoV-2 inoculation. Both parameters were recorded from days 0 to 12 post infection (pi). The mean ± SD is presented. A Mann-Whitney U test was conducted to compare differences in weight between the two groups on day 12 (n = 9-12 animals per group) (**P < 0.01). Kaplan-Meier survival curves were generated (n = 6-9 animals per group) and the P value was calculated using the [log-rank (Mantel-Cox) test] (*P < 0.05). (c) Viral load (genome equivalent/µg RNA) and viral infectious particle units (PFU/mg of tissue) in the lungs of mock-vaccinated (grey) and vaccinated (blue) hCD40/K18-hACE2 transgenic mice (n = 3 animals per group) on day 5 pi with the median plotted as a line. (d) Levels of IgG antibodies (AU) binding to Wuhan and VOCs SARS-CoV-2 RBD proteins before vaccination (baseline, -2 days post-vaccination (dpv), n = 9-12 animals per group), after the completion of the vaccination schedule (28 dpv, n = 9-12 animals per group), and 40 dpv (i.e., day 12 pi time point, n = 3-5 animals per group). (e) Levels of IgG antibodies (AU) binding to SARS-CoV-2 (circles) and SARS-CoV-1 (triangles) S proteins in mock-vaccinated (grey) and vaccinated (blue) animals at -2, 28, and 40 dpv. Medians [Min-Max] are shown. The grey dashed lines represent prime and boost vaccines. The red dashed line represents SARS-CoV-2 inoculation. Neutralizing activity of (f) anti-RBD antibodies (units/mL) and (g) anti-S antibodies (units/mL) in mock-vaccinated (grey) and vaccinated (blue) animals post-vaccination (open circles) and post-infection (solid circles). Medians ± Interquartile ranges (IQRs) are shown. Thirty plasma samples from unvaccinated mice were used to determine the threshold for positivity, defined as the whole units/mL value immediately above the concentration of the highest sample for RBD (i.e., 8 units/mL) and Spike (i.e., 4 units/mL) proteins. These results were reproduced in a second independent experiment (Figure S3).

Figure 3. CD40.CoV2 and mRNA BNT162b2 vaccines elicit similar cross-reactive and neutralizing antibody responses. Levels of IgG antibodies (AU) binding to Wuhan and VOCs SARS-CoV-2 RBD proteins (α, β, γ, δ, Omicron) (a) and neutralizing activity of anti-RBD antibodies (percentage of inhibition relative to the Wuhan RBD protein) (b) one week after completion of the vaccination schedule in BNT162b2 mRNA (red) or CD40.CoV2 vaccinated animals (blue) (n=5 and 20 animals, respectively). Medians ± Interquartile ranges (IQRs) are shown.

Figure 4. Determination of the optimal immunogenic CD40.CoV2 vaccine concentration and proliferation of specific T cells induced by the CD40.CoV2 vaccine. (a) Gating strategy for specific T cells that upregulate activation-induced markers (AIM). (b) Antigen specific activation of $CD4^+$ (blue) and $CD8^+$ (green) T cells from COVID-19 convalescent patients (n = 5) stimulated with various concentrations of CD40.CoV2 vaccine or a combination of OLPs covering the full-length sequence of the vaccine antigens (vOLPmix). Activation of SARS-CoV-2-specific $CD4^+$ and $CD8^+$ T cells is shown as the percentage of $CD69^+$ $CD137^+$ cells within the $CD4^+$ or $CD8^+$ subset after background subtraction. Median values (solid line) ± interquartile ranges (IQRs) (dashed lines) are shown. (c) Gating strategy for assessing the proliferation of specific T and B cells after seven days of CD40.CoV2 stimulation. (d) Proliferation of $CD4^+$ T-cells, $CD8^+$ T-cells, and B-cells from COVID-19 convalescent patients (n = 10) induced by the CD40.CoV2 vaccine, an irrelevant vaccine (CD40 Gp140z [1 nM]), or an equimolar concentration of vOLPmix. Data are expressed as a proliferation index obtained by dividing the frequency of proliferating cells after specific stimulation over background. Median values ± IQRs are shown. [Friedman and Dunn's multiple comparison tests] were used for statistical analysis (**P < 0.01, ***P < 0.001).

Figure 5. Heatmap of standardized biomarker expression in culture supernatants induced by the CD40.CoV2 vaccine. Supernatants from convalescent COVID-19 patient PBMCs collected on day 2 after stimulation with the CD40.CoV2 vaccine (1 nM) or an equimolar concentration of vOLPmix (n = 15). The

colors represent standardized expression values centered around the mean, with variance equal to 1. Biomarker hierarchical clustering was computed using the Euclidean distance and Ward's method.[72]

Figure 6. Polyfunctional and cytotoxic specific T-cell responses of convalescent COVID-19 patients after *in-vitro* stimulation with the CD40.CoV2 vaccine. (a) Representative dot plots of SARS-CoV-2-specific $CD4^+$ and $CD8^+$ T-cell responses after in vitro stimulation of patient PBMCs with the CD40.CoV2 vaccine (1 nM) on D0 and re-stimulation with various vOLPs (vRBD, vS1, vS2 or vN2) (1 µg/ml) on D8. (b) Functional composition of SARS-CoV-2-specific $CD4^+$ and $CD8^+$ T-cell responses induced by the CD40.CoV2 vaccine and various vOLPs (vRBD, vS1, vS2 or vN2) (1 µg/ml). Responses are color coded according to the combination of cytokines produced. The arcs identify cytokine-producing subsets (IFN-γ, IL-2, and TNF) within the $CD4^+$ or $CD8^+$ T cell populations. (c) Frequency and radar charts of the merged median of IFN-γ^+ SARS-CoV-2-specific $CD4^+$ (blue) or $CD8^+$ (green) T cells from convalescent COVID-19 patients (n = 14) stimulated or not with the CD40.CoV2 vaccine (1 nM) on D0 and re-stimulated with various vOLPs (vRBD, vS1, vS2 or vN2), cont.OLP (SARS-CoV-2 N1-N2, or Ebola Gpz) (grey) on D8 (1 µg/mL). Median values ± IQRs are shown. [Friedman and Dunn's multiple comparison tests] were used for statistical analysis (*P < 0.05, **P < 0.01, ***P < 0.001, ****P < 0.0001, ns: not significant). (d) Specific lysis of $CD8^+$ T cells stimulated with the CD40.CoV2 vaccine (1 nM) against autologous PHA-blasted PBMCs from five different convalescent COVID-19 patients, pulsed with either vRBD (light green), vN2 (dark green), or cont.OLP (SARS-CoV-2 N1-N2 or M) (grey). The means of triplicate values ± the standard deviation (SD) are shown. Each symbol represents a different patient.

Figure 7. Polyfunctional specific T-cell responses against SARS-CoV-2 VOCs after stimulation with the CD40.CoV2 vaccine. Frequency of total cytokines (IFN-γ ± IL-2 ± TNF) produced by specific $CD4^+$ (blue) or $CD8^+$ (green) T cells from convalescent COVID-9 patients (n = 18) after i*n-vitro* stimulation with the CD40.CoV2 vaccine (1 nM) on D0 and re-stimulation with RBD OLP from various VOCs/VOI (a) or RBD OLP from Omicron VOC (n = 13) (1 µg/mL) (b). Functional composition of SARS-CoV-2-specific $CD4^+$ and $CD8^+$ T-cell responses induced by the CD40.CoV2 vaccine against VOCs/VOI. Responses are color coded according to the combination of cytokines produced. The arcs identify cytokine-producing subsets (IFN-γ, IL-2, and TNF) within the $CD4^+$ and $CD8^+$ T-cell populations (c). Median values ± IQRs are shown. [Friedman's test] and [Wilcoxon U test] were used for comparisons (*P < 0.05, **P < 0.01, ***P < 0.001, ****P < 0.0001).

Figure 8. Cross-reactive specific T-cell responses against SARS-CoV-1 and MERS of convalescent COVID-19 patients after *in-vitro* stimulation with the CD40.CoV2 vaccine. Frequency of total cytokines (IFN-γ ± IL-2 ± TNF) produced by specific $CD4^+$ (blue) or $CD8^+$ (green) T cells after *in-vitro* stimulation with the CD40.CoV2 vaccine (1 nM) on D0 and re-stimulation with OLPs representing the sequences of S1, vRBD, and vN2 from (a) SARS-CoV-1 and (b) S1 from MERS (1 µg/mL). Median values ± IQRs are shown. The [Wilcoxon U test] was used for comparisons (**P < 0.01, ***P < 0.001, ns: not significant).

a

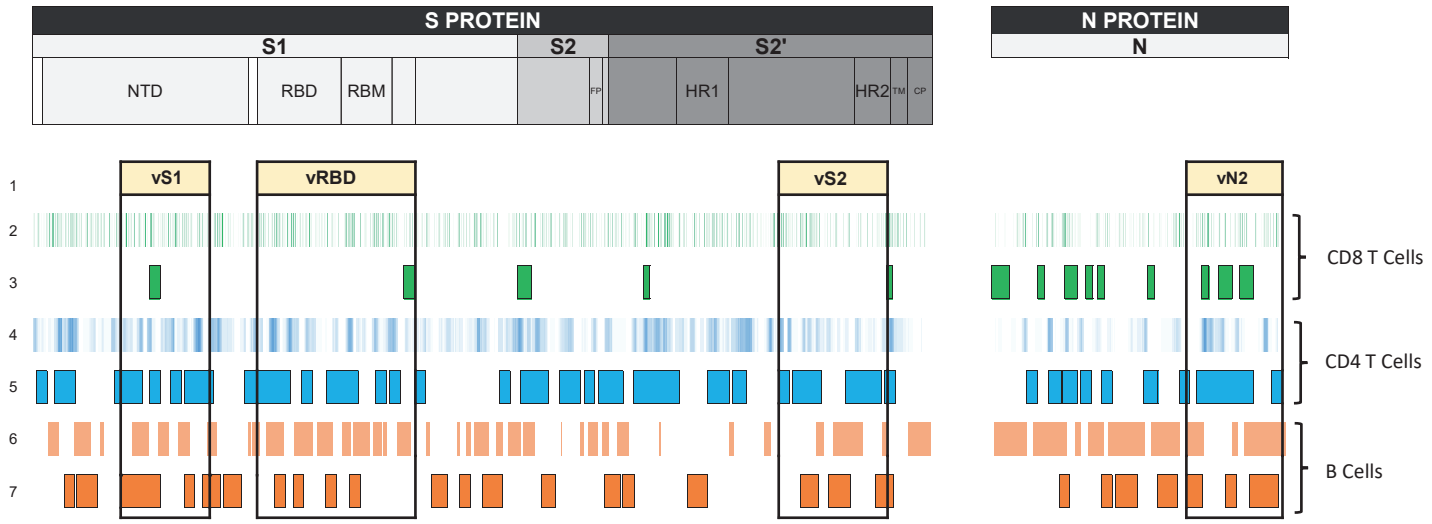
S PROTEIN
S1
S2
S2'
NTD
RBD
RBM
FP
HR1
HR2
TM
CP
N PROTEIN
N
vS1
vRBD
vS2
vN2
1
2
3
4
5
6
7
CD8 T Cells
CD4 T Cells
B Cells

b

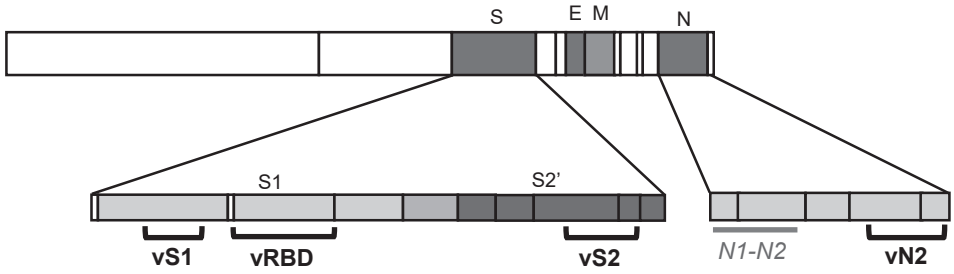
S
E
M
N
S1
S2'
vS1
vRBD
vS2
N1-N2
vN2

c

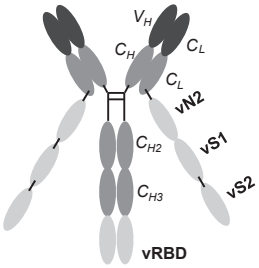
V_H
C_H
C_L
C_L
vN2
C_{H2}
vS1
vS2
C_{H3}
vRBD

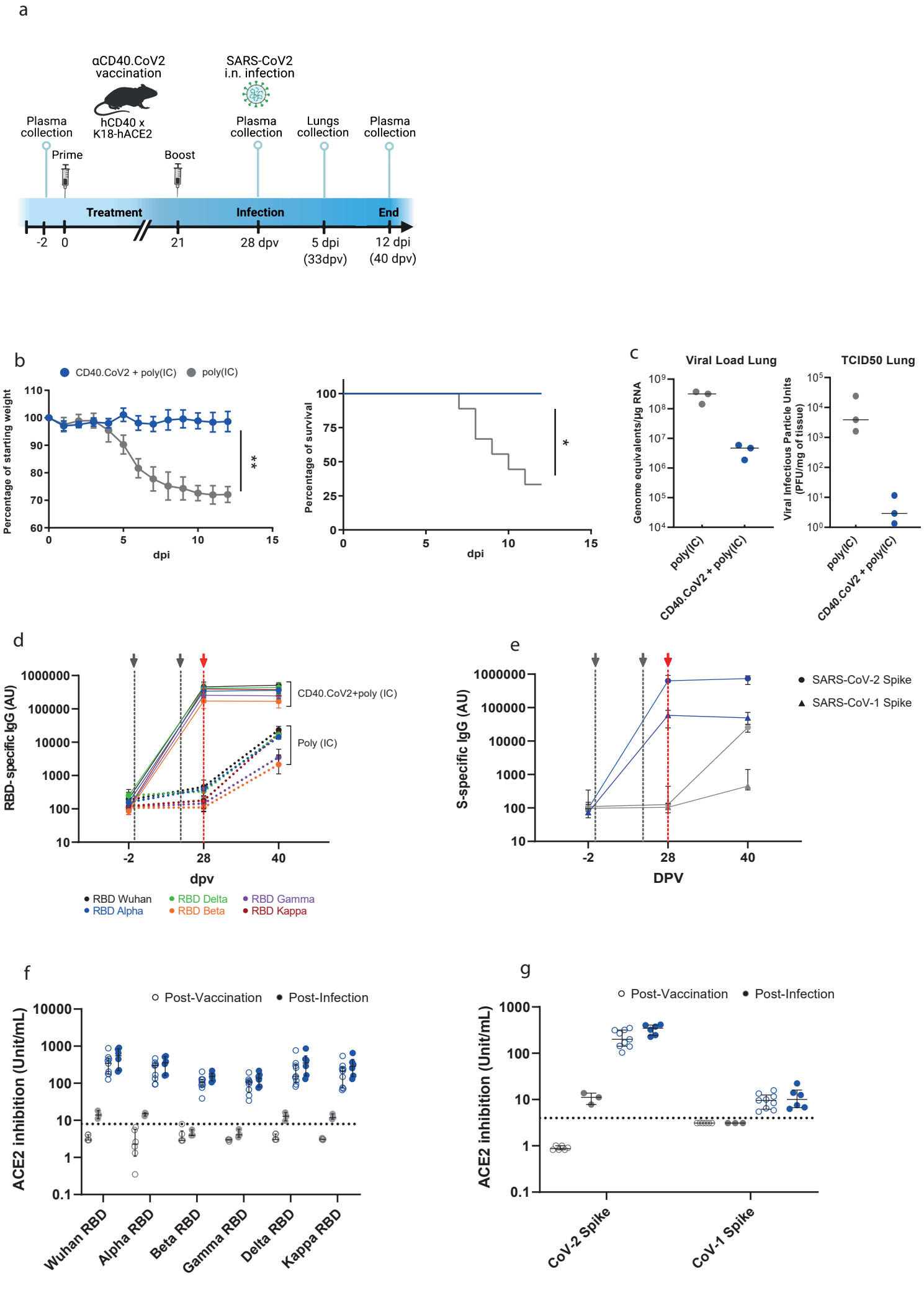
a
αCD40.CoV2 vaccination
hCD40 x K18-hACE2
SARS-CoV2 i.n. infection
Plasma collection
Prime
Boost
Plasma collection
Lungs collection
Plasma collection
Treatment
Infection
End
-2
0
21
28 dpv
5 dpi (33dpv)
12 dpi (40 dpv)
b
CD40.CoV2 + poly(IC)
poly(IC)
Percentage of starting weight
dpi
**
Percentage of survival
dpi
*
c
Viral Load Lung
Genome equivalents/µg RNA
poly(IC)
CD40.CoV2 + poly(IC)
TCID50 Lung
Viral Infectious Particle Units (PFU/mg of tissue)
poly(IC)
CD40.CoV2 + poly(IC)
d
RBD-specific IgG (AU)
CD40.CoV2+poly (IC)
Poly (IC)
dpv
RBD Wuhan
RBD Alpha
RBD Delta
RBD Beta
RBD Gamma
RBD Kappa
e
S-specific IgG (AU)
SARS-CoV-2 Spike
SARS-CoV-1 Spike
DPV
f
Post-Vaccination
Post-Infection
ACE2 inhibition (Unit/mL)
Wuhan RBD
Alpha RBD
Beta RBD
Gamma RBD
Delta RBD
Kappa RBD
g
Post-Vaccination
Post-Infection
ACE2 inhibition (Unit/mL)
CoV-2 Spike
CoV-1 Spike

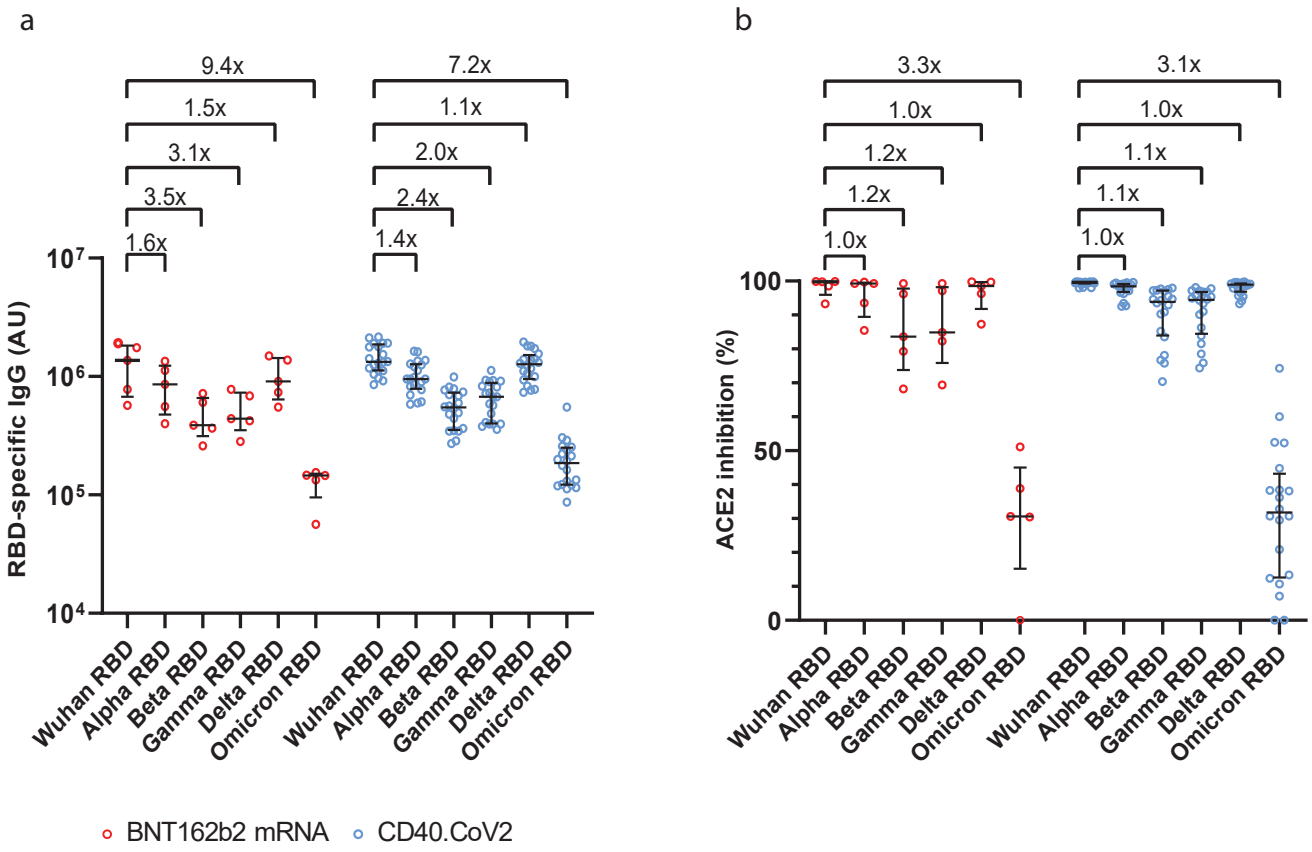
a
b
9.4x
1.5x
3.1x
3.5x
1.6x
7.2x
1.1x
2.0x
2.4x
1.4x
RBD-specific IgG (AU)
10^7
10^6
10^5
10^4
3.3x
1.0x
1.2x
1.2x
1.0x
3.1x
1.0x
1.1x
1.1x
1.0x
ACE2 inhibition (%)
100
50
0
Wuhan RBD
Alpha RBD
Beta RBD
Gamma RBD
Delta RBD
Omicron RBD
BNT162b2 mRNA
CD40.CoV2

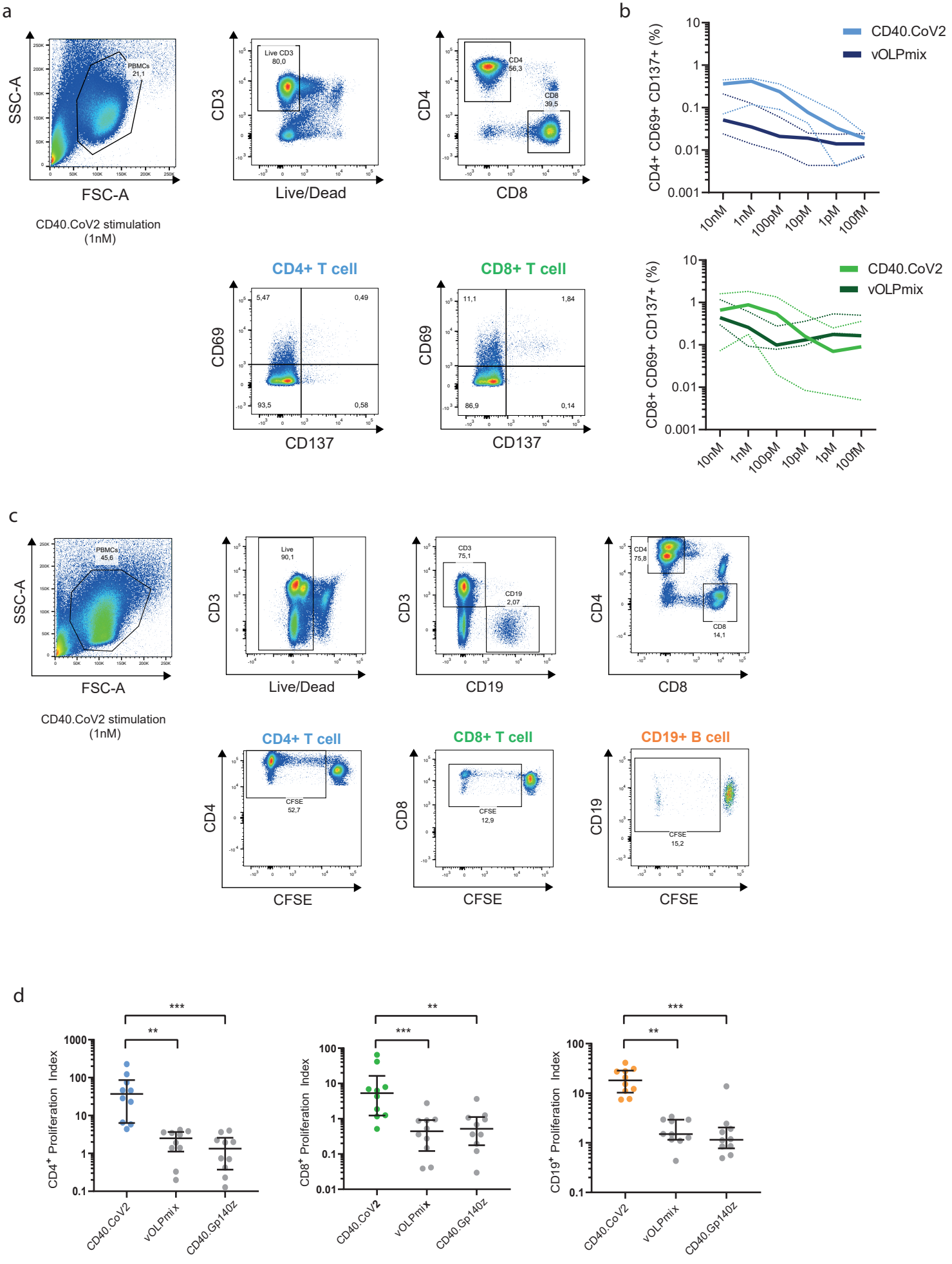
a
SSC-A
FSC-A
PBMCs
21,1
CD40.CoV2 stimulation
(1nM)
CD3
Live/Dead
Live CD3
80,0
CD4
CD8
CD4
56,3
CD8
39,5
CD4+ T cell
CD8+ T cell
CD69
CD137
5,47
0,49
93,5
0,58
11,1
1,84
86,9
0,14
b
CD4+ CD69+ CD137+ (%)
CD8+ CD69+ CD137+ (%)
CD40.CoV2
vOLPmix
10nM
1nM
100pM
10pM
1pM
100fM
c
PBMCs
45,6
Live
90,1
CD19
CD3
75,1
2,07
CD4
75,8
CD8
14,1
CD4+ T cell
CD8+ T cell
CD19+ B cell
CFSE
52,7
12,9
15,2
d
CD4+ Proliferation Index
CD8+ Proliferation Index
CD19+ Proliferation Index
CD40.CoV2
vOLPmix
CD40.Gp140Z

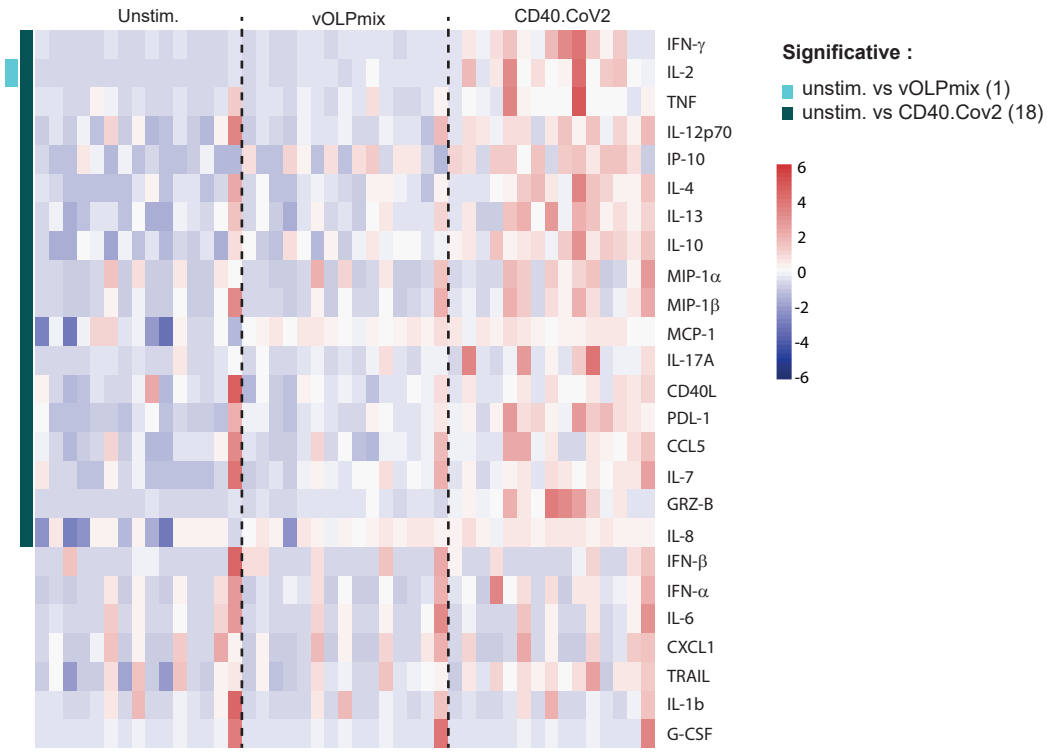
Unstim.
vOLPmix
CD40.CoV2
IFN-γ
IL-2
TNF
IL-12p70
IP-10
IL-4
IL-13
IL-10
MIP-1α
MIP-1β
MCP-1
IL-17A
CD40L
PDL-1
CCL5
IL-7
GRZ-B
IL-8
IFN-β
IFN-α
IL-6
CXCL1
TRAIL
IL-1b
G-CSF
Significative :
unstim. vs vOLPmix (1)
unstim. vs CD40.Cov2 (18)
6
4
2
0
-2
-4
-6

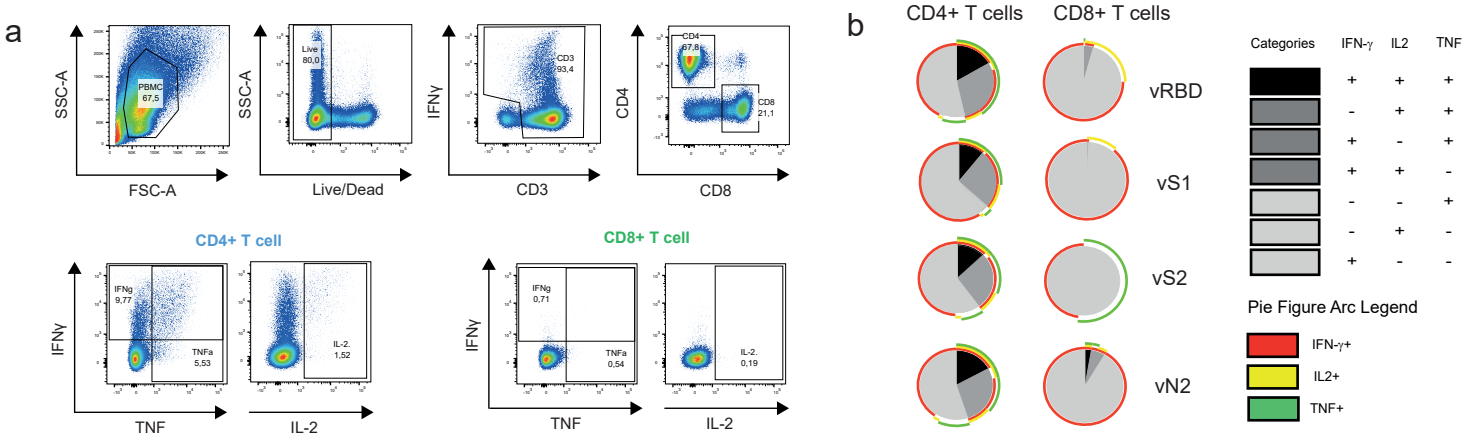

Stimulation D0: CD40.CoV2 (1nM)
Re-stimulation D8: vRBD (1 µg/ml)

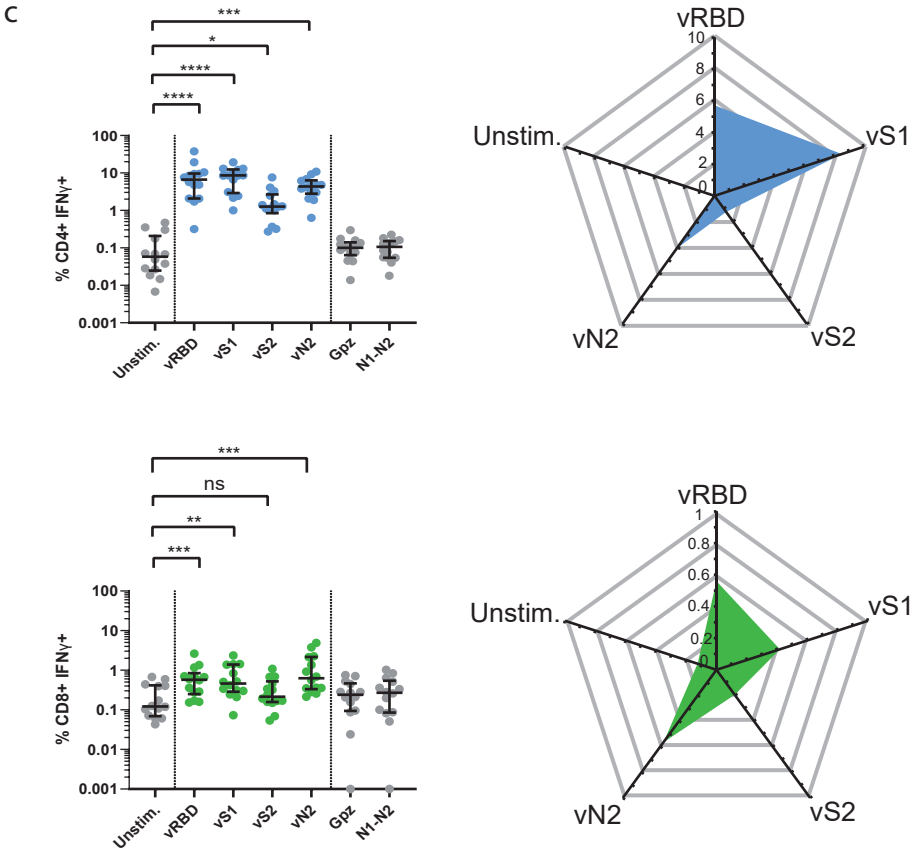

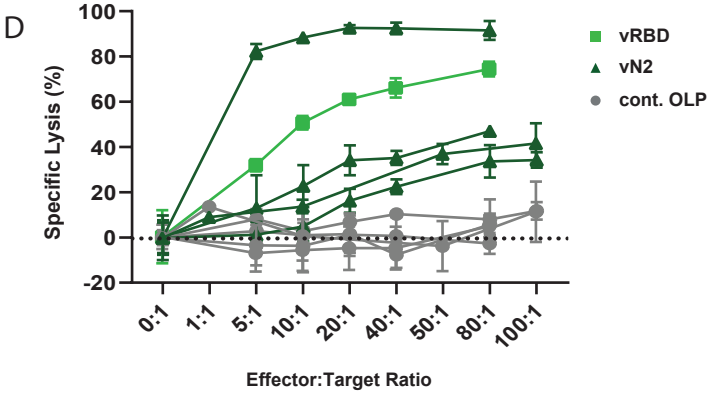

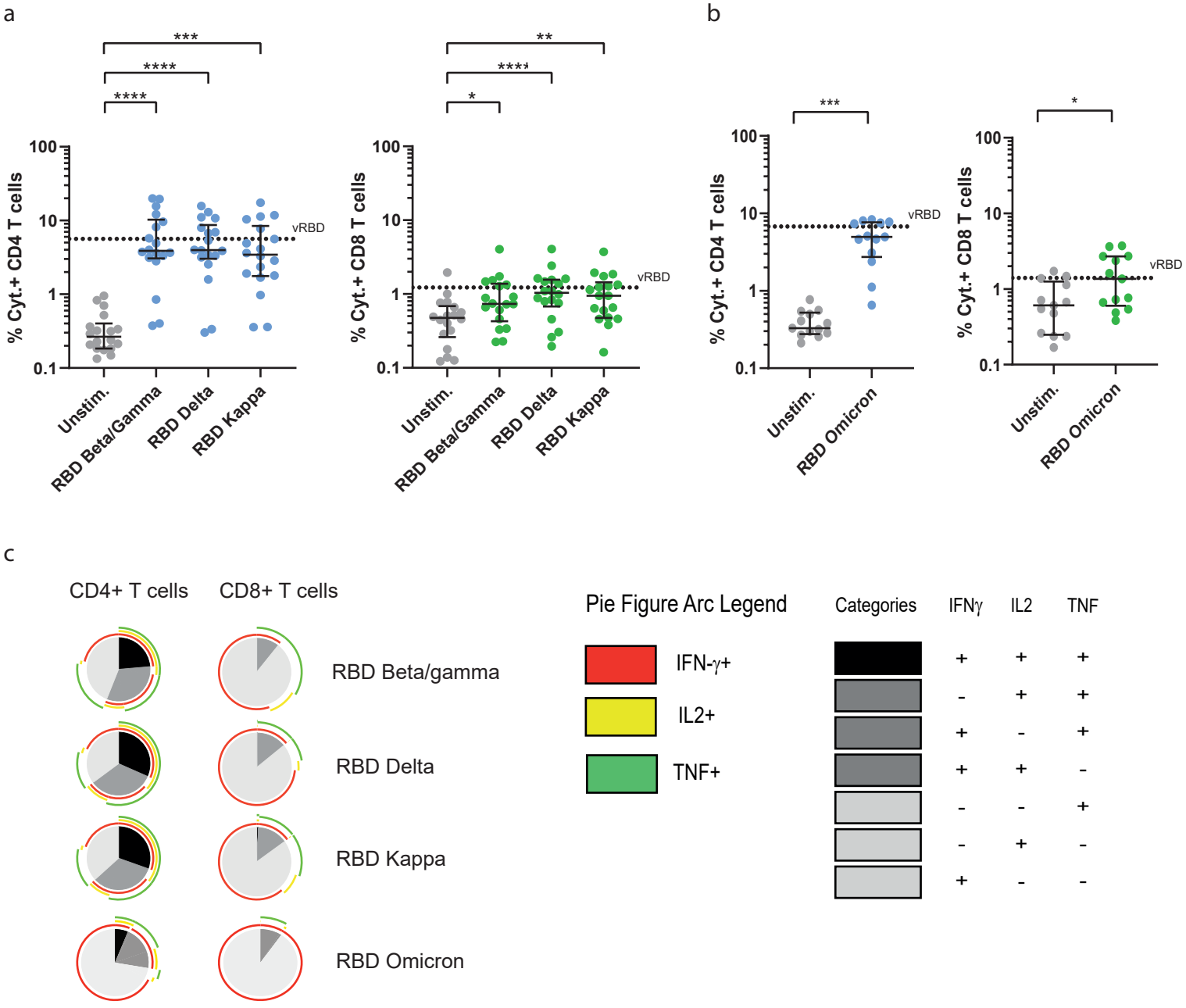
a
b
c
% Cyt.+ CD4 T cells
% Cyt.+ CD8 T cells
vRBD
Unstim.
RBD Beta/Gamma
RBD Delta
RBD Kappa
RBD Omicron
CD4+ T cells
CD8+ T cells
RBD Beta/gamma
RBD Delta
RBD Kappa
RBD Omicron
Pie Figure Arc Legend
IFN-γ+
IL2+
TNF+
Categories
IFNγ
IL2
TNF

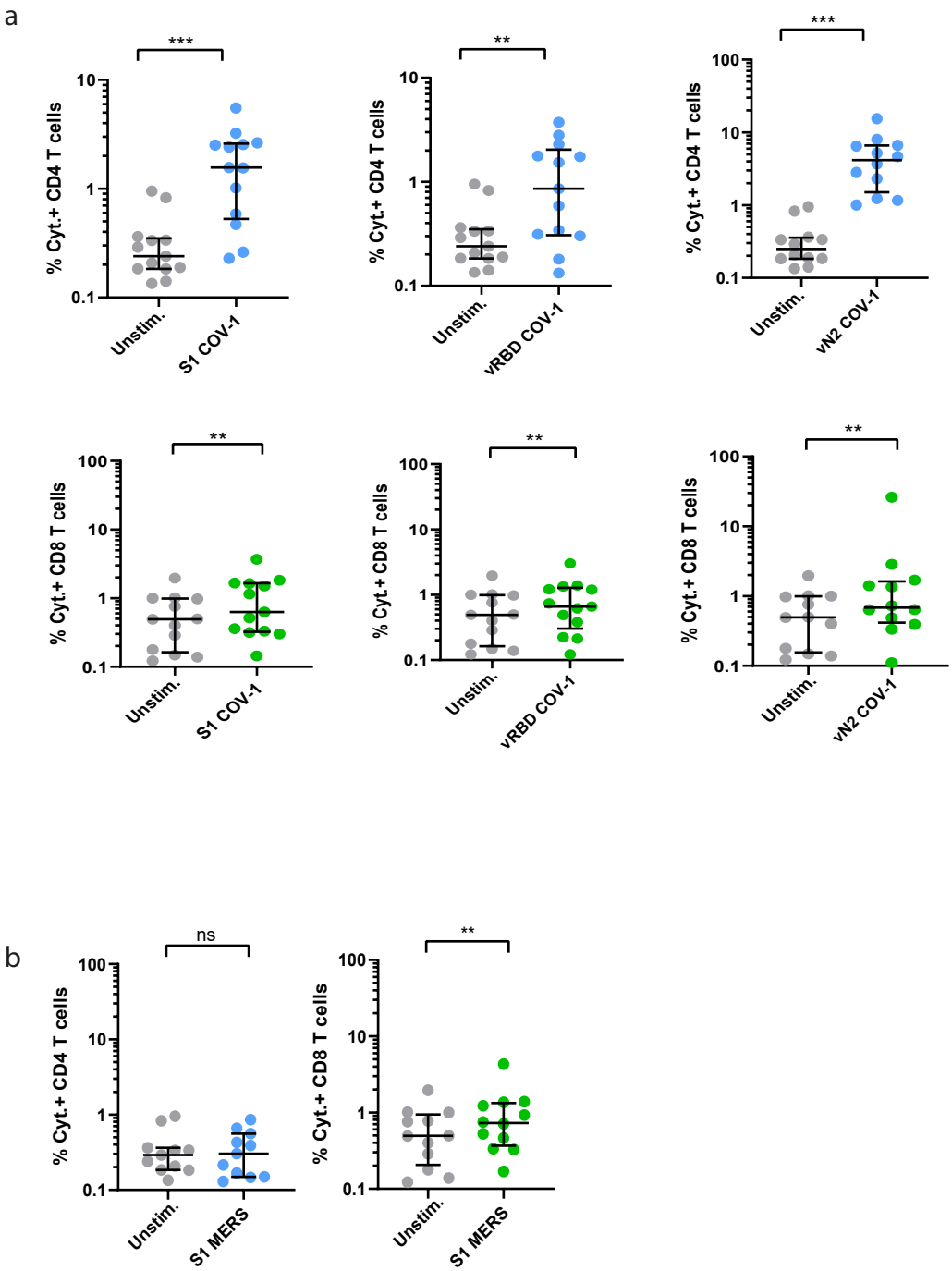
a
***
**
***
% Cyt.+ CD4 T cells
10
1
0.1
Unstim.
S1 COV-1
vRBD COV-1
vN2 COV-1
100
% Cyt.+ CD8 T cells
b
ns
S1 MERS